AN INTEGRATED APPROACH TO STRATIGRAPHIC ARCHITECTURE AND RESERVOIR ANALYSIS OF THE EUTAW FORMATION: EASTERN GILBERTOWN FIELD, ALABAMA

By

BRADLEY JOSEPH JACKSON

Bachelor of Science in Geology

Oklahoma State University

Stillwater, Oklahoma

2013

Submitted to the Faculty of the
Graduate College of the
Oklahoma State University
in partial fulfillment of
the requirements for
the Degree of
MASTER OF SCIENCE
May, 2017

AN INTEGRATED APPROACH TO STRATIGRAPHIC ARCHITECTURE AND RESERVOIR ANALYSIS OF THE EUTAW FORMATION: EASTERN GILBERTOWN FIELD, ALABAMA

Thesis Approved:

Dr. Jack Pashin

Thesis Adviser

Dr. James Puckette

Dr. Daniel Lao Davila

ACKNOWLEDGEMENTS

I would like to thank my advisor Dr. Pashin for never hesitating to help me on my work or answering a question I had, as well as enabling me to do this project, it has opened many doors to future possibilities. Dr. Puckette, not only for being on my committee, but for being so passionate about geology and investing so much into your students, and for being a critical part of my academic career at OSU. Dr. Davila and Dr. Mohamed for taking part as committee members, and the entire Geology department. I would also like to thank the Geological Survey of Alabama for the resources needed to complete this project.

Lastly and most importantly, thank you to my amazing family; my mother and father, brother and sisters, nieces and nephews, cousins, aunts and uncles, and grandparents. To my beautiful wife, Christine, thank you for believing in me and for always encouraging me during this process and everything I do in life. The Lord has truly blessed me with a family that supports me in anything I do in my life, everything I have and have accomplished is because of my family, and I am extremely thankful for that.

Name: BRADLEY JOSEPH JACKSON

Date of Degree: MAY, 2017

Title of Study: AN INTEGRATED APPROACH TO STRATIGRAPHIC ARCHITECTURE AND RESERVOIR ANALYSIS OF THE EUTAW FORMATION: EASTERN GILBERTOWN FIELD

Major Field: GEOLOGY

Abstract: The Gilbertown Oil Field in Choctaw County, Alabama is the oldest commercial oil field in the state. Today the field is extremely mature and is at risk of abandonment. More than 85% of the oil produced in Gilbertown Field is from glauconitic sandstone of the Cretaceous-age Eutaw Formation. The Eutaw Formation comprises 7 major reservoir units dominated by glauconitic sandstone. This sandstone constitutes low-resistivity, low-contrast pay that is difficult to characterize using conventional geophysical log analysis. Highly conductive minerals such as glauconite and siderite, which make up as much as 30% of the reservoir rock, are the primary reason for the low resistivity pay zones in the Eutaw Formation. The primary goal of this study is to employ an integrated approach that utilizes wireline log analysis, core analysis, and thin section analysis to characterize the stratigraphic architecture and reservoir quality of the Eutaw Formation at Gilbertown Field. The results of this analysis could be crucial for guiding the future development of the oil field and for avoiding premature abandonment. The central hypothesis of this research is that the low resistivity signatures in wireline logs of the Eutaw Formation can obscure hydrocarbon-bearing zones, thus increasing the potential for bypassed pay. The eastern part of Gilbertown Oil Field has produced nearly 12 MMbbl of oil from the Eutaw Formation since initial development in 1945. An integrated method for volumetric analysis and pay evaluation in the eastern part of the field resulted in an estimated 82.4 MMbbl of original oil-in-place in the Eutaw Formation. To date, less than 15% of this oil has been recovered, and geological analysis indicates that the potential for improving recovery and revitalizing Gilbertown Field is high.Type the abstract here. Limit 350 words, single spaced.

TABLE OF CONTENTS

LIST OF TABLES

Table Page

LIST OF FIGURES

Figure Page

Figure Page

CHAPTER I

INTRODUCTION

The Gilbertown Oil Field in Choctaw County, Alabama was discovered in 1944 and is home to the first commercial oil well in Alabama. This discovery marked the beginning of major exploration and development in the state and resulted in the establishment of the State Oil and Gas Board of Alabama. The Carter Oil Company drilled the Eutaw Formation discovery well in Gilbertown Field, the Sam Alman No. 1 well in Sec. 5, T. 10 N., R. 3 E., in August of 1945. The well was drilled on surface geological data following the discovery of oil in fractured chalk of the Selma Group on the basis of seismic prospecting the year before (Current, 1948; Frascogna, 1957). Reservoir energy for the field is a natural water drive, and water and oil are the main fluids produced in the field. Today the field is extremely mature and is at risk of abandonment. The vast majority of the oil produced in Gilbertown Field is from Cretaceous-age sandstone of the Eutaw Formation. An earlier study of Gilbertown Field (Pashin et al., 2000), which focused primarily on the Selma chalk reservoir, stated that a need exists for an in-depth assessment of the petrology and reservoir characteristics of the Eutaw sandstone reservoirs, particularly in the eastern part of the field where Eutaw production has been most prolific and where large volumes of unswept oil may remain.

Reservoirs of the Eutaw Formation are dominated by glauconitic sandstone that constitutes low-resistivity, low-contrast pay, thus using conventional geophysical log analysis for reservoir characterization is very difficult (Pashin et. al., 2000). The low-resistivity pay problem

makes the quantification of water saturation (Sw) from wireline logs extremely difficult, because calculated Sw values are unrealistically high if the reservoir does not conform to the assumptions required for standard petrophysical evaluation of clean or shaly formations (Worthington, 2000). Low-resistivity, low-contrast pay exists where there is a lack of contrast between what are normally highly resistive hydrocarbon-bearing zones and low resistivity water-bearing zones (Worthington, 2000). High residual water saturation in pay zones compounds this issue. Pay being defined as portions of reservoir that contain economically producible hydrocarbons. Characterizing low-resistivity pay is a problem that has been observed in basins all over the world, especially in marine deposits containing conductive verdine minerals, such as glauconite, chlorite, and chamosite.

Glauconite and siderite, which make up as much as 30% of the Eutaw reservoir rock, are the primary reason for the low resistivity pay zones in Gilbertown Field (Pashin et al., 2000). A vintage (1944-1960) log suite comprising mainly electric logs with only spontaneous potential and resistivity curves contributes to difficulty characterizing pay. This is because alternate methods for pay characterization in low resistivity sandstone require density and neutron porosity logs, which are available only from a few wells drilled during redevelopment of the field by the Belden and Blake Corporation in the mid-1970s.

Commercial core analyses from the Eutaw Formation at Gilbertown are valuable because they provide independent, laboratory-derived values for porosity, permeability, water saturation, and oil saturation. These analyses provide the key to developing a robust pay analysis procedure that can help quantify original oil-in-place (OOIP) and remaining oil-in-place (ROIP), and developing this procedure is the main objective of this study. Production and completion data that are available through the State Oil and Gas Board of Alabama assist in the identification and characterization of pay zones and are instrumental for calculating remaining oil-in-place and understanding why specific zones were selected for completion. My objective is to better

understand these parameters to provide insight into the heterogeneity of the sandstone and the potential identification of untapped pay.

The primary goal of this study is to employ an integrated approach that utilizes wireline log analysis, core analysis, and thin section analysis to characterize the stratigraphic architecture and reservoir quality of the Eutaw Formation at Gilbertown Field. The results of this analysis may prove crucial for guiding the future development and prolonging the life of the oil field. The central hypothesis of this investigation is that the low resistivity zones in wireline logs of the Eutaw Formation contain untapped or bypassed hydrocarbon pay zones. This hypothesis can be tested using the commercial core analyses in tandem with the available geophysical log suite to develop a robust pay analysis procedure for the Eutaw Formation that can help quantify remaining resources with greater accuracy than previous efforts. Petrographic thin section analysis further helps test this hypothesis by facilitating quantification the proportion of verdine minerals in the zones of interest and their potential effect on log response.

CHAPTER II

BACKGROUND

Gilbertown Field is located in Choctaw County, southwest Alabama, within the peripheral fault system along the northern margin of the Mississippi Interior Salt Basin (Pashin et al., 2000), a rifted basin that formed during the opening of the Gulf of Mexico during the Mesozoic-Cenozoic (Salvador, 1987; Worrall and Snelson, 1989) (Figs.1 and 2). Eastern Gilbertown Field is developed in a faulted anticline and horst restricted on the north by the Gilbertown Fault System and on the south by the West Bend fault system. Rifting was initiated following extensional collapse of the Appalachian-Ouachita Orogen near the beginning of the Mesozoic (Horton et al., 1984). As rifting gave way to passive margin development, evaporite sedimentation and consequent salt tectonic activity following the main rifting phase had a serious impact on the structural and sedimentological evolution of the region, which ultimately affected the generation and entrapment of hydrocarbons (Salvador, 1987; Pashin et al., 2000).

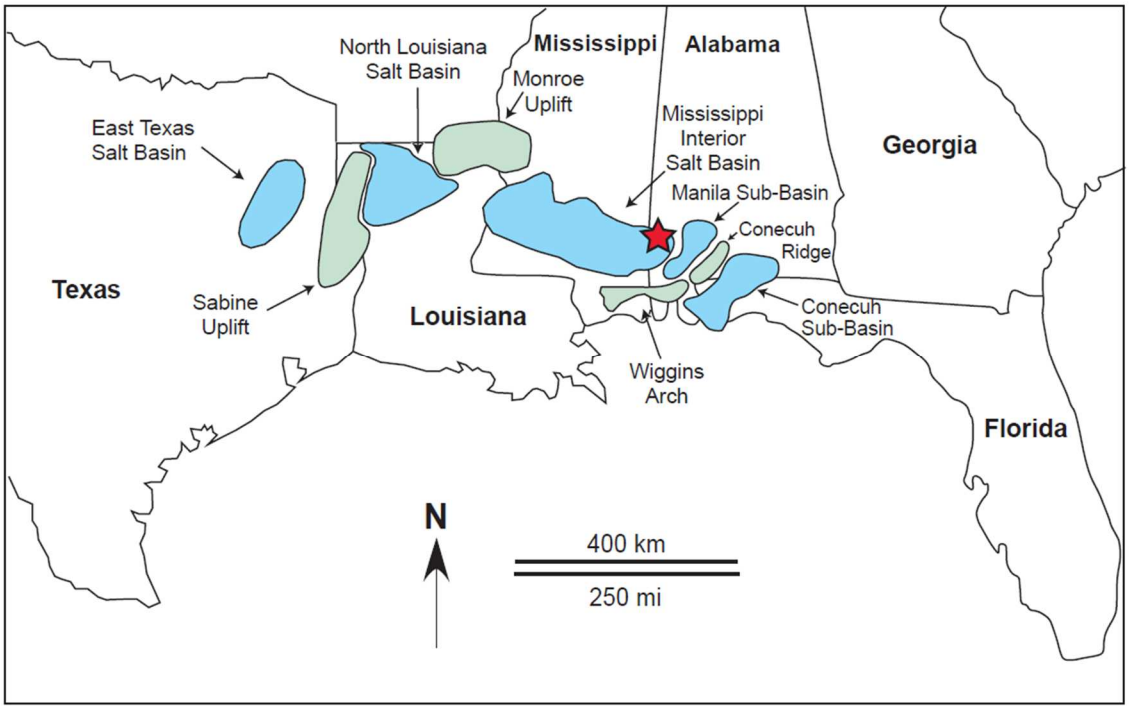

Figure 1. Map showing location of interior salt basins and subbasins in the north central and northeastern Gulf of Mexico area. Approximate location of Gilbertown Field marked by red star (modified from Mancini et al., 2005)

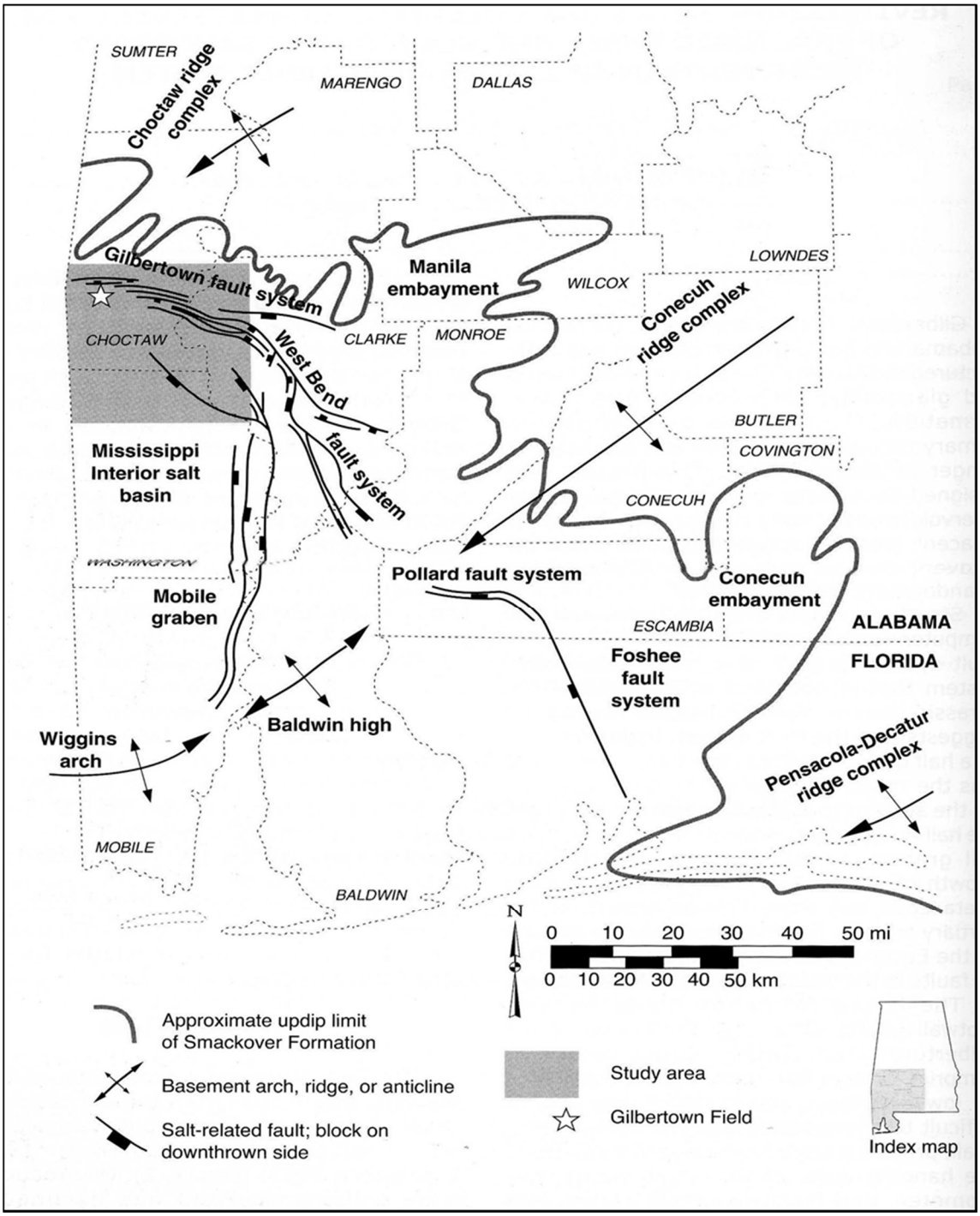

Figure 2. Structural features in the Gulf Coast basin of southwest Alabama with location of study area and Gilbertown Field (modified from Mann and Kopaska-Merkel, 1990).

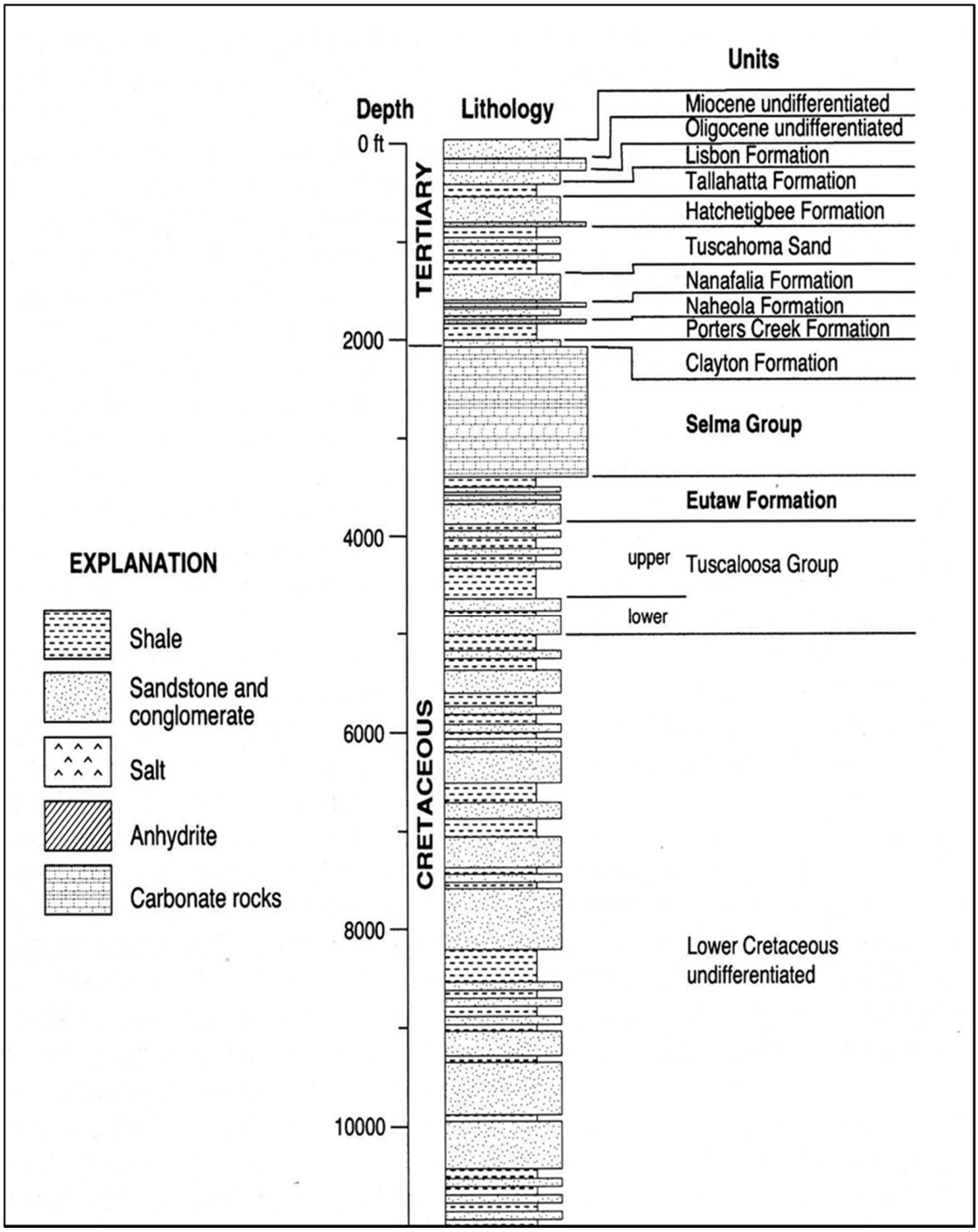

Figure 3. Generalized stratigraphic section showing Cretaceous-Tertiary (Paleogene Period) stratigraphy in Gilbertown Field and adjacent areas (modified from Pashin et al., 2000).

Due to the absence of continuous core, identification of bedding successions and sedimentary structures is not possible; however, the Eutaw Formation in other areas of Alabama and Mississippi has been characterized as transgressive beach and shelf deposits (Frazier and Taylor, 1980; Cook, 1993; Greer, 1995; Pashin et al., 2000). The Eutaw Formation was likely deposited on the inner continental shelf, due to the sands being fine grained and deposited as widespread blankets (Greer, 1995). Mollusk shells and foraminifera tests in cuttings and core chips confirm deposition in marine environments, and so a beach or shelf interpretation is appropriate (Pashin et al., 2000). Pashin et al. (2000) also noted wheatseed siderite, which is suggestive of subaerial alteration of the sandstone units. The Eutaw Formation, which overlies the Tuscaloosa Group in Gilbertown Field, contains up to 290 feet of interbedded sandstone and shale and fines upward into chalk of the Selma Group above (Fig.3).

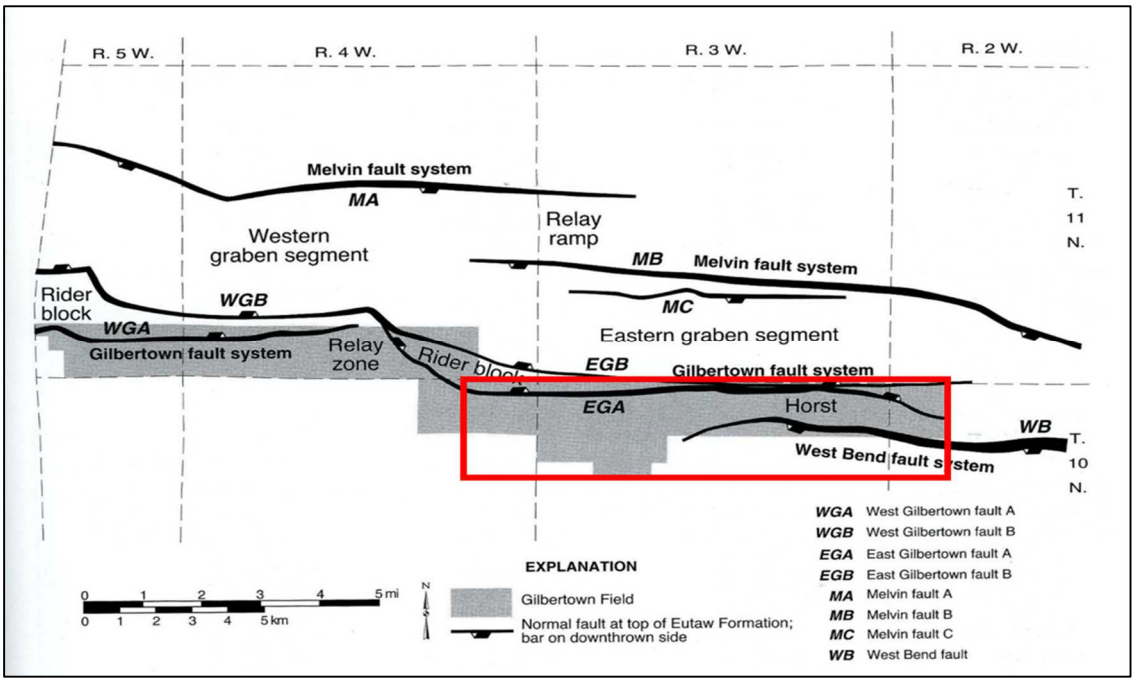

Figure 4. Map showing faults in Gilbertown Field. Red box outlines study area in eastern Gilbertown Field (modified from Pashin et al., 2000)

The Eutaw Formation can be subdivided into seven stratigraphic units by fieldwide shale markers that have been interpreted as marine flooding surfaces (Pashin et al., 2000). The eastern part of Gilbertown Field produces primarily from the Eutaw Formation in structural traps in the faulted anticline and the horst between East Gilbertown Fault A (EGA) and the West Bend fault system (WB) (Fig. 4). Area balanced structural cross-sections constructed by Pashin et al. (1998) indicate synsedimentary growth of these structures from early Cretaceous through Tertiary (Paleogene Period) time. Seal analysis indicates that Eutaw oil production is restricted to footwall uplifts where shale and sandstone are juxtaposed with impermeable chalk; smeared Eutaw sand and shale likely contribute to seal integrity (Pashin et al., 2000). It also is important to note that Gilbertown Field is a heavy oil field, producing oil with a gravity of 17-19° API. The low mobility of heavy oil may be a key factor limiting efficient drainage of the reservoirs.

Several studies describe the structure of the area in detail, characterizing and modeling the faults of the field primarily for the revitalization of the Selma chalk reservoir (Pashin et al., 1998; Qi et al., 1998; Jin et al., 1999; Jin and Groshong, 2006; Jin et al., 2009). The study of Pashin et al. (2000) focused primarily on characterizing the fractured reservoirs in the Selma Chalk, and so they did not perform a complete characterization of the Eutaw Formation. Their contributions however, laid the groundwork for this study. Extensive structural and net sandstone isolith mapping was performed that establishes the relationships between the structure of the Eutaw Formation and the intervals that were perforated. Critical observations are that there is no simple oil-water contact in the Eutaw Formation, that hydrodynamic trapping and localized leakage along the fault may be responsible for the irregular distribution of oil in the Eutaw Formation, and that cementation is a major source of reservoir heterogeneity. The study notes that intervals that were perforated in some wells were not necessarily perforated in neighboring wells, although there were no obvious differences in log characteristics. They recognized the difficulty of performing conventional log analysis on the Eutaw sands with a very limited suite of geophysical well logs and performed a basic statistical analysis of the available commercial core

analyses. They commented that the field has outstripped reserve estimates repeatedly, which suggests that there is still significant bypassed pay that can be discovered by using the integrated methods being proposed in this study.

A study of the Eutaw Formation in Mississippi was completed by Greer (1995), who discussed increasing oil production from glauconitic sandstone by secondary recovery methods. His study area was along the peripheral faults just west of Gilbertown Field in Clarke County, Mississippi, where the fields produce the same type of heavy oil as in Gilbertown Field. Other studies of the low-resistivity sands of the Eutaw Formation in Mississippi demonstrate that there is great potential for overlooked and bypassed pay. Cook et al. (1990) performed a study in Mississippi that resulted in the discovery of 100 Bcf of bypassed gas pay at Trimble Field. They integrated conventional core measurements, gas detection equipment on mudlogging units, and electric logging suites consisting of a dual induction spherically focused log, a lithodensity-compensated neutron-density log, gamma ray log, and the electromagnetic propagation tool. Although they possessed a more extensive set of resources than were deployed in Gilbertown Field, many aspects of their approach appear to be transferrable.

CHAPTER III

METHODOLOGY

Characterizing the Eutaw reservoirs in eastern Gilbertown Field employed a diverse suite of methods. A geophysical log suite consisting mainly of SP and resistivity curves was analyzed stratigraphically and petrophysically. In the eastern Gilbertown Field, 133 wells have geophysical logs that penetrate the top of the Selma Group. Of those, 108 wells penetrate the top of the Eutaw Formation, and 32 penetrate the top of the Tuscaloosa Group. Correlations were made by slipping logs and comparing patterns in the SP and resistivity curves. Units correlated include the top of the Selma Group, the top of the Eutaw Formation, the seven internal intervals when applicable, and lastly the top of the Tuscaloosa Group.

The SP curves were used to determine the net thickness of sandstone in each interval of the Eutaw Formation and also played an important role in determining the original oil-in-place. Two stratigraphic cross sections were constructed using the top of the Eutaw Formation as a datum that traverse the field from west to east, parallel to faults EGA and WB. These cross sections display the stratigraphic architecture, completed zones, and oil-saturated sandstone zones identified in core analyses. Area balanced cross-sections were constructed by Pashin et al. (1998; 2000). Two of these structure cross sections, which are perpendicular to faults EGA and WB have been redrawn to enhance the view of the Eutaw oil accumulation in eastern Gilbertown Field. Two structural cross sections were constructed using the same wells as the stratigraphic cross sections to show the productive zones and the potential bypassed zones that are behind pipe. The structure and stratigraphic cross sections used the same approach as was used in

Pashin et al., (2000) to display the different parameters.

The shaly sandstone techniques of Walsh et al. (1993) and low-resistivity, low-contrast pay methods described in Asquith (1990) were also attempted to test whether more advanced methods of pay characterization are applicable to the Eutaw Formation in Gilbertown. The no porosity compensation shaly sandstone method described by Walsh et al. (1993) and Asquith (1990) requires only SP and resistivity logs and corrects water saturation and porosity values in clay-bearing reservoir sandstone, which seemed ideal for the vintage log suite of Gilbertown Field. Other methods described in Asquith (1990) require a more advanced set of well logs, and as there are very few wells with porosity logs in Gilbertown Field, these methods could not be used.

Core analyses from nine wells are on file at the State Oil and Gas Board of Alabama and were used for statistical analysis of reservoir properties. Owing to the difficulty of log analysis alone, the core analyses were instrumental for developing a robust reservoir analysis method for computing SoPhiH ((1-water saturation) * porosity * thickness) and original oil-in-place (OOIP). Pashin et al., (2000), performed a basic statistical analysis for each interval in the Eutaw Formation using core analysis data. Statistics include geometric means, maxima, minima, standard deviations, and standard errors for oil saturation, porosity, and permeability. The analysis, however, only included samples with oil saturation values greater than zero. Statistics derived in this study include lognormal averages of water saturation, porosity, and permeability values for each interval for each well where core analysis was available. Oil saturation values vary greatly, and oil saturated zones are always adjacent to zones with zero oil saturation; therefore arithmetic averages were used for oil saturation values of each interval in each well. All wells discussed in this thesis are identified by the State Oil and Gas Board of Alabama permit number (i.e., well 206).

Numerous maps were constructed during this study. Structure maps, isopach maps, and net sandstone isolith maps were initially hand contoured. These maps were then digitized into

Petra software for further evaluation. Only wells drilled through the entire interval were used for mapping interval and net sandstone thickness. Maps of geometric mean core analysis parameters, such as oil saturation, water saturation, and porosity were gridded and contoured for each interval using Petra. These maps employed a grid size of 200 feet x 200 feet (xy units) and the "highly connected features" surface style and gridding algorithm. The grid size and algorithm were determined by trial and error to determine what resulted in the most realistic interpretation, and the 200 feet x 200 feet grid size is a fine grid, and is approximately 25% of the average well spacing. Wells with acoustic logs were utilized to calculate and map porosity after being corrected for shale volume using the methods from Asquith (1990). Due to the spotty coverage of oil and water saturation data, wells with no core analysis that were above the oil-water contact for each interval were populated with the geometric means from the data available. SoPhiH maps were then contoured using grid-to-grid calculations in Petra to combine the net sandstone, porosity, and water saturation maps. The SoPhiH values below the oil-water contact for each interval equal zero according to the core analysis data. Maps of OOIP were constructed using the grid calculations, using the equation (7,758 * SoPhiH * Area/Bo) combined with the SoPhiH maps and original oil-in-place values for each interval were determined using the volumetric tab in Petra.

Production and completion data were compiled from the Oil and Gas Board of Alabama's database, which was accessed online (http://ogb.state.al.us). Production decline curve analysis of wells and producing units were used to calculate the recovery efficiency of the wells and the field. A production bubble map was made showing cumulative production of wells perforated in the Eutaw Formation and those values were used in conjunction with the OOIP results to calculate the percent recovery, shown in a bubble map. There are also maps showing attributes such as perforated intervals and dates wells were drilled. Completion data were used to analyze how intervals chosen for completion targets vary across eastern Gilbertown Field and were integrated with other results to establish why the targets vary so greatly. The completion data

used in conjunction with structure maps of each interval resulted in the finding of the lowest known elevation of production or the structural production limit for each interval.

The oil-water contacts were determined by combining the production and completion data, the core analysis and, and the structural contour map of each interval. Wells with core analysis were the basis for determining the elevation of lowest known oil where available, however scarce or inconclusive data required the integration of production and completion data. If there was no indication that the interval was oil saturated in the core analysis, production, or completion data then that depth structurally would be considered below the oil-water contact.

Thin sections of Eutaw sandstone from core chips were made available by the Geological Survey of Alabama and were used to aid in assessing framework sandstone composition, provenance, diagenesis, depositional environment, and reservoir quality. Thin sections are available from all Eutaw sandstone intervals except E1, and each thin section was impregnated with blue epoxy to highlight porosity and was stained with alizarin red-S to help identify calcite and with potassium ferricyanide to identify potassium feldspar and iron-bearing minerals. A petrographic microscope was used to describe, photograph, and point count each thin section. Point counts were conducted by analyzing six views per slide with fifty counts per view. This resulted in 300 counts per slide to use for analysis and interpretation of framework sandstone composition, provenance, and diagenesis. The results helped quantify the distribution of verdine minerals and calcite cement, which have a large effect on reservoir heterogeneity. Point counting also helped to verify lab-determined porosity values.

CHAPTER IV

RESULTS

Structural Geology

Mapping the structure of the Eutaw Formation demonstrates the geometry of the oil trap in Gilbertown Field. The highest elevation of the Eutaw Formation is -2,980 feet and is adjacent to Fault EGA opposite the tip region of Fault WB (Fig. 5). Fault EGA dips north, whereas Fault WB dips south (Fig. 6). The dip of the faults is approximately 60° in Eutaw and older strata and decreases to ~45° in the Selma Group and the overlying Tertiary (Paleogene Period) section (Pashin et al., 1998). Cross section A-A' is a north-south dip section that traverses Faults EGA and WB that displays the geometry of the Eutaw trap as a faulted footwall anticline. Here, the oil

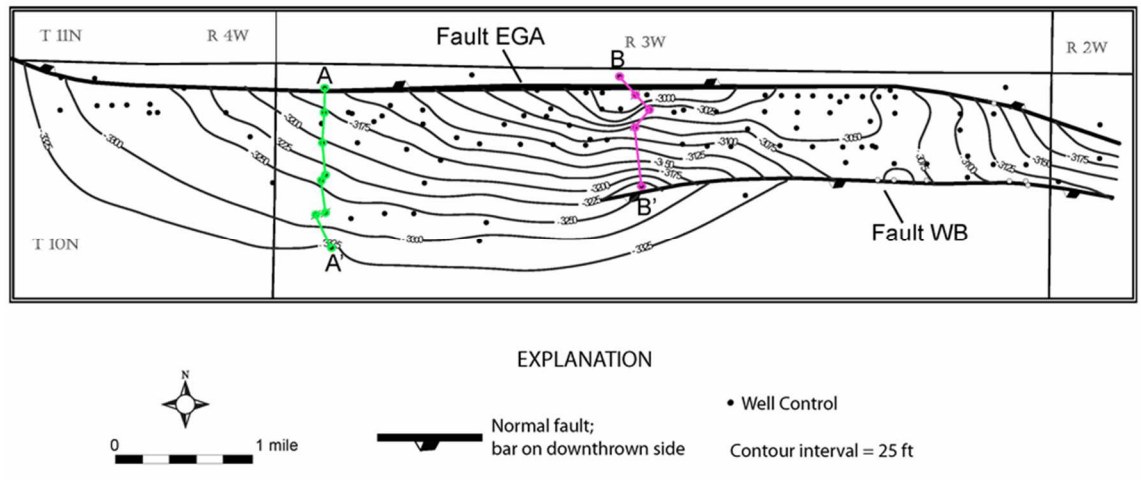

Figure 5. Structural contour map of the top of the Eutaw Formation showing location of structural cross sections A-A' and B-B'.

accumulation is restricted to the upper part of the Eutaw Formation and is bounded by Fault EGA. Cross section B-B' traverses the central and structurally highest part of eastern Gilbertown Field and shows the trap as a horst in which the Eutaw oil accumulation is bounded by both faults.

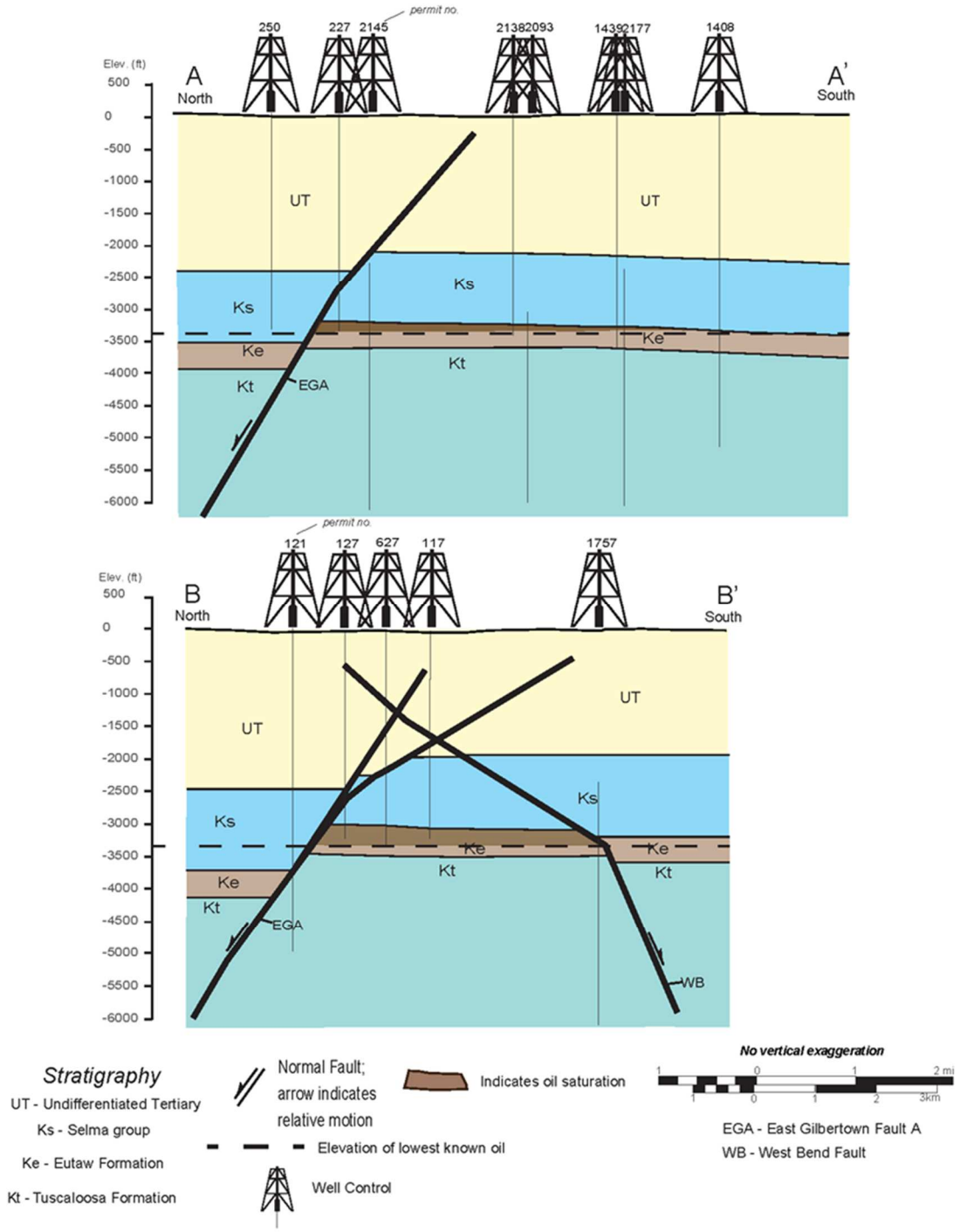

Figure 6. Structural cross sections A-A' and B-B' showing geometry of the oil trap in eastern Gilbertown Field. See Figure 5 for location.

Stratigraphic Architecture

The stratigraphic cross sections and type log for the Eutaw Formation in the Gilbertown area display the stratigraphic architecture of the intervals within the Eutaw Formation, as well as the typical log signatures seen on the SP and resistivity curves (Figs. 7, 8). The contact between the Eutaw Formation and the Tuscaloosa Group can be difficult to recognize, and in many instances, the formation boundary appears to be arbitrary (Figs. 7, 8). However, the sandstone units of the Tuscaloosa Group typically form a coarsening-upward succession, and the Eutaw Formation forms an overall fining-upward succession. Although the Eutaw Formation forms an overall fining upward succession, the log signature of each constituent sandstone unit is distinctive. The shallow and deep resistivity curves in the Eutaw Formation tend to track one another at approximately 1 ohm, with the exception of shallow resistivity spikes in low porosity intervals (Figs. 7, 8).

Interval E1 typically has a coarsening-upward to blocky log signature (Fig. 7). Interval E2 tends to coarsen upward and contains two stacked sandstone bodies (Fig. 7). Intervals E3 and E4 contain sandstone that intertongues with shale, however interval E3 coarsens upward from shale to sandstone and interval E4 tends to fine upwards from sandstone to shale, clean sand bodies are apparent in both intervals (Fig. 7). Interval E5 is a shaly interval that coarsens upward into sandstone near the top of the interval and has a higher shale to sandstone ratio than interval E4 (Fig. 7). Interval E6 consists of a series of interbedded shale and sandstone units. There is predominantly a shale section at the base that coarsens into a sandstone interval which then fines into a shaly sandstone with prominent sandstone at the top of the interval (Fig. 7). However, SP response is highly variable and shows a distinct serrate log signature, indicating that this interval has signficant lateral variability of clay and glauconite content (Fig. 7). The uppermost interval of the Eutaw Formation is interval E7 and is made up of mostly sandstone and forms a prominent sandstone body (Fig. 7). The Eutaw Formation is sharply overlain by the Selma Group, which

has much higher resistivity patterns and lower SP signatures that contrast strongly with Eutaw strata (Fig. 7) (Pashin et al., 2000).

Cross sections C-C' and D-D' demonstrate the changes in SP and resistivity log characteristics as well as changes in interval thickness and net sandstone thickness across the map area (Fig. 8). Perforated zones and zones saturated with oil and water further show the variability of the distribution of completion targets. Isopach maps of intervals E1 through E7 are shown in Figures 9 and 10. Maps of net sandstone thickness are shown in Figures 11 and 12.

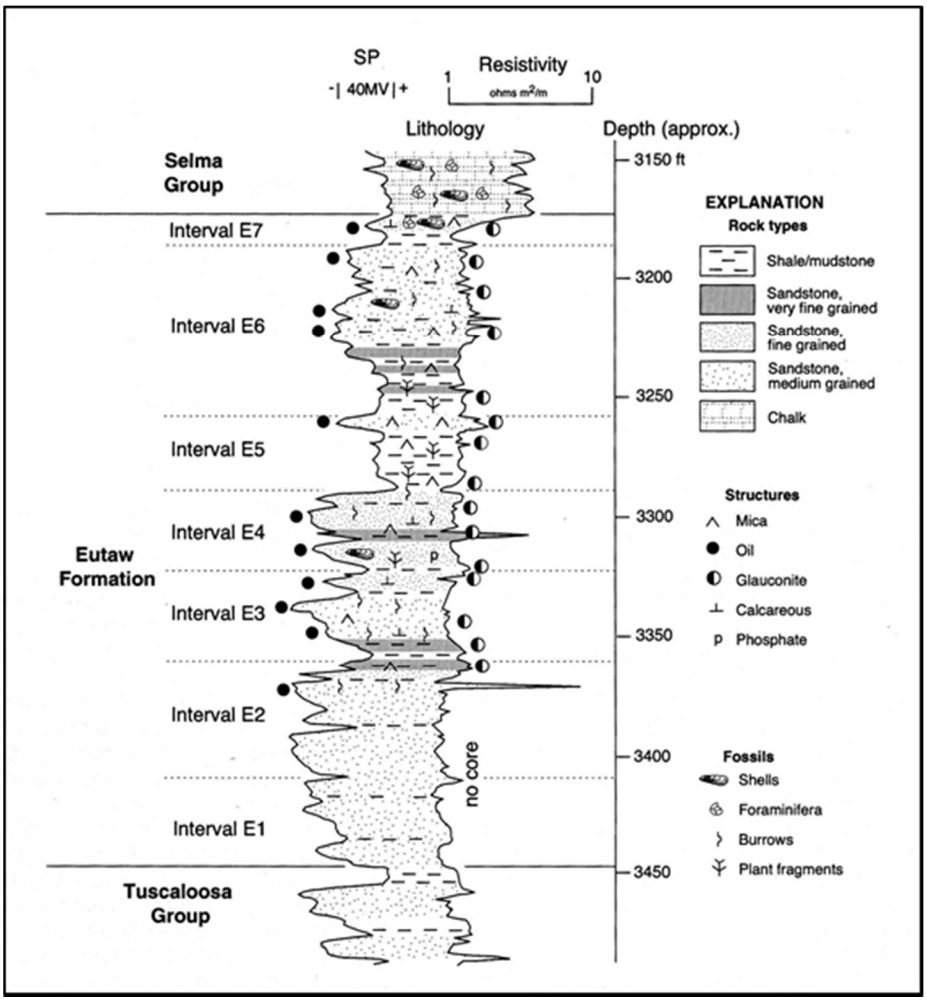

Figure 7. Composite section and geophysical well log of the Eutaw Formation in Gilbertown Field (after Pashin et. al., 2000).

Cook (1993) reported that the basal Eutaw sandstone is coarse grained and contains gravel with phosphate nodules at the base of an area updip of Gilbertown Field. Interval E1 is the least sampled interval by geophysical well logs; it has a coarsening-upward SP signature in the western portion of the map area (Fig. 8). The SP signature becomes blockier in the horst between faults EGA and WB, and has a higher shale content near fault EGA. Interval thickness ranges from less than 40 feet in the faulted anticline west of the horst to greater than 50 feet in the horst where it has the blocky SP signature (Figs. 8 and 9). Sandstone in interval E1 averages 30 feet in thickness, it thins to less than 25 feet near Fault EGA in the west of the map area and is consistently 30 feet to greater than 35 feet in the faulted anticline and the horst (Fig. 11).

Interval E2 is approximately 40 to 50 feet thick in the horst and is thicker than 65 feet in the faulted anticline (Fig. 9). Sandstone thickness in interval E2 averages 36 feet, and it is less than 25 feet in the faulted anticline west of the horst and is locally thicker than 40 feet in the horst (Fig. 11). The sandstone in the horst has a strong, negative SP deflection which could indicate low clay content and high porosity (Fig. 8).

Interval E3 ranges in thickness from 30 to 50 feet, and there is no obvious thickness trend (Fig. 9). Sandstone thickness in interval E3 averages 26 feet and ranges from less than 25 feet in the structurally lowest part of the faulted anticline and is locally thicker than than 30 feet thick within the faulted anticline (Fig. 11). The interval has a consistent coasening-upward SP signature throughout the map area, but it does become shalier in the horst near the faults (Fig. 8).

Interval E4 also varies in thickness from 30 to 50 feet, and the interval thins toward the highest part of the eastern Gilbertown structure (Fig. 9). The fining upward SP signature is consistent acrossed the map area, however in many of the wells there are two distinct sandstone units, a thin one at the base and a thicker, fining upward sandstone at the top of the interval (Fig. 8). Sandstone in interval E4 is thicker than 30 feet in the southwestern part of the map area. The

sandstone thins toward the top of the faulted anticline and is consistently thinner than 25 feet in the horst Fig. (11).

Interval E5 averages 40 feet in thickness, and values range from less than 35 feet in the faulted anticline to more than 45 feet in the eastern horst (Fig. 10). Sandstone thickness in interval E5 averages only 12 feet, constituting only 30% of the total interval. The sandstone is thicker than 20 feet off structure to the southwest, and thins toward the structurally highest part of the horst, where it is less than 10 feet thick (Fig. 12). The SP pattern of the sandstone in interval E5 has a strong negative deflection west and east of the horst, whereas the interval has a suppressed SP response and thus is very shaly in the highest part of the horst (Fig. 8).

E6 is the thickest interval in the Eutaw Formation, averaging 65 feet thick and ranging from less than 55 feet west of the structure and thickening to more than 75 feet on the east side of the horst (Fig. 10). Net sandstone thickness in interval E6 averages nearly 60 feet, but as mentioned before, the sandstone has a serrate SP logprofile, indicating that it is shaly (Fig. 8). Overall, the sandstone thickens toward the highest part of the structure from 40 to 60 feet (Fig. 12). Sandstone is consistently 45 to 55 feet thick in the horst, with the exception of two areas adjacent to Faults EGA and WB, where the sandstone is less than 45 feet thick (Fig. 12). Like interval E5, SP patterns in interval E6 indicate that the reservoir has elevated shale content in the highest parts of the structure (Fig. 8).

Interval E7 is the thinnest interval in the formation, averaging only 11 feet in thickness and pinching out the structurally highest part of the field adjacent to Fault EGA (Fig. 10). The interval is thickest in the southwest where maximum values exceed 25 feet. Net sandstone thickness in interval E7 ranges from 0 to 15 feet and pinches out in areas adjacent to Fault EGA on the horst (Fig. 12). Net sandstone thickness averages only 6 feet, and the sandstone is thicker than 15 feet in the western part of the map area (Fig. 12). The SP signature of the sandstone is very inconsistent in the central part of the horst, and negative deflection is most pronounced off structure in the western part of the map area (Fig. 8).

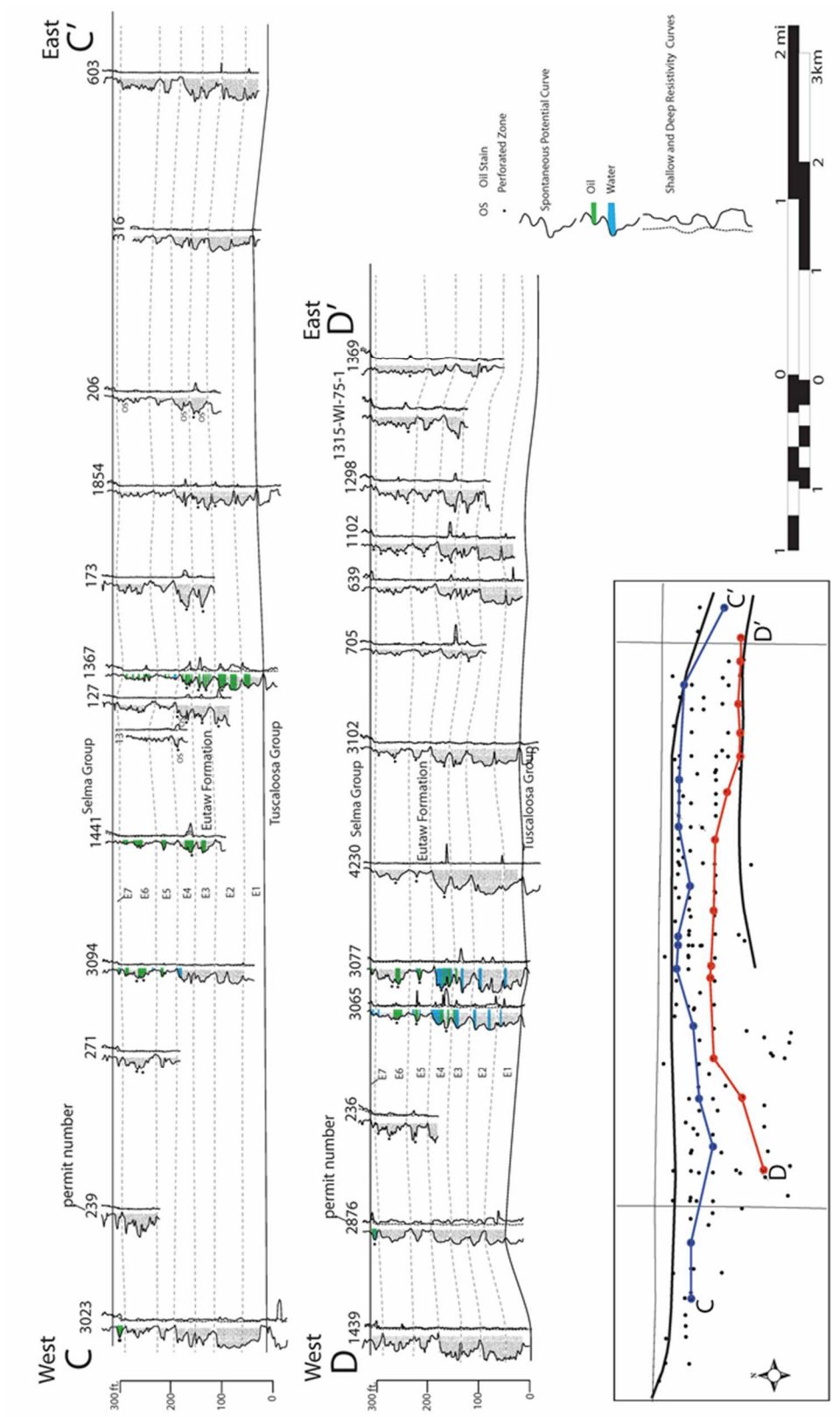

Figure 8. Stratigraphic cross sections of the Eutaw Formation, eastern Gilbertown Field. Map showing location of cross sections C-C' and D-D'.

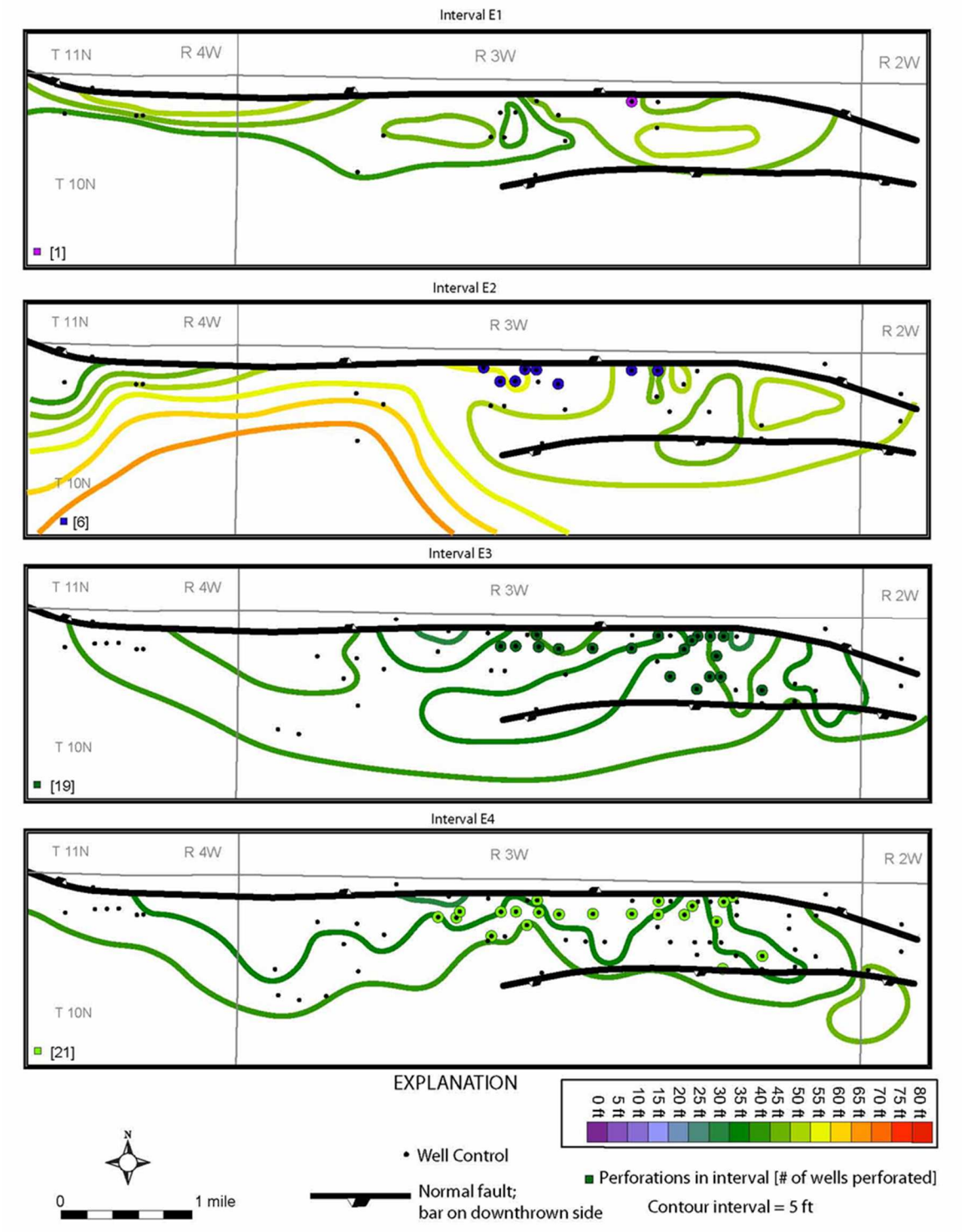

Figure 9. Isopach maps of intervals E1-E4, eastern Gilbertown Field.

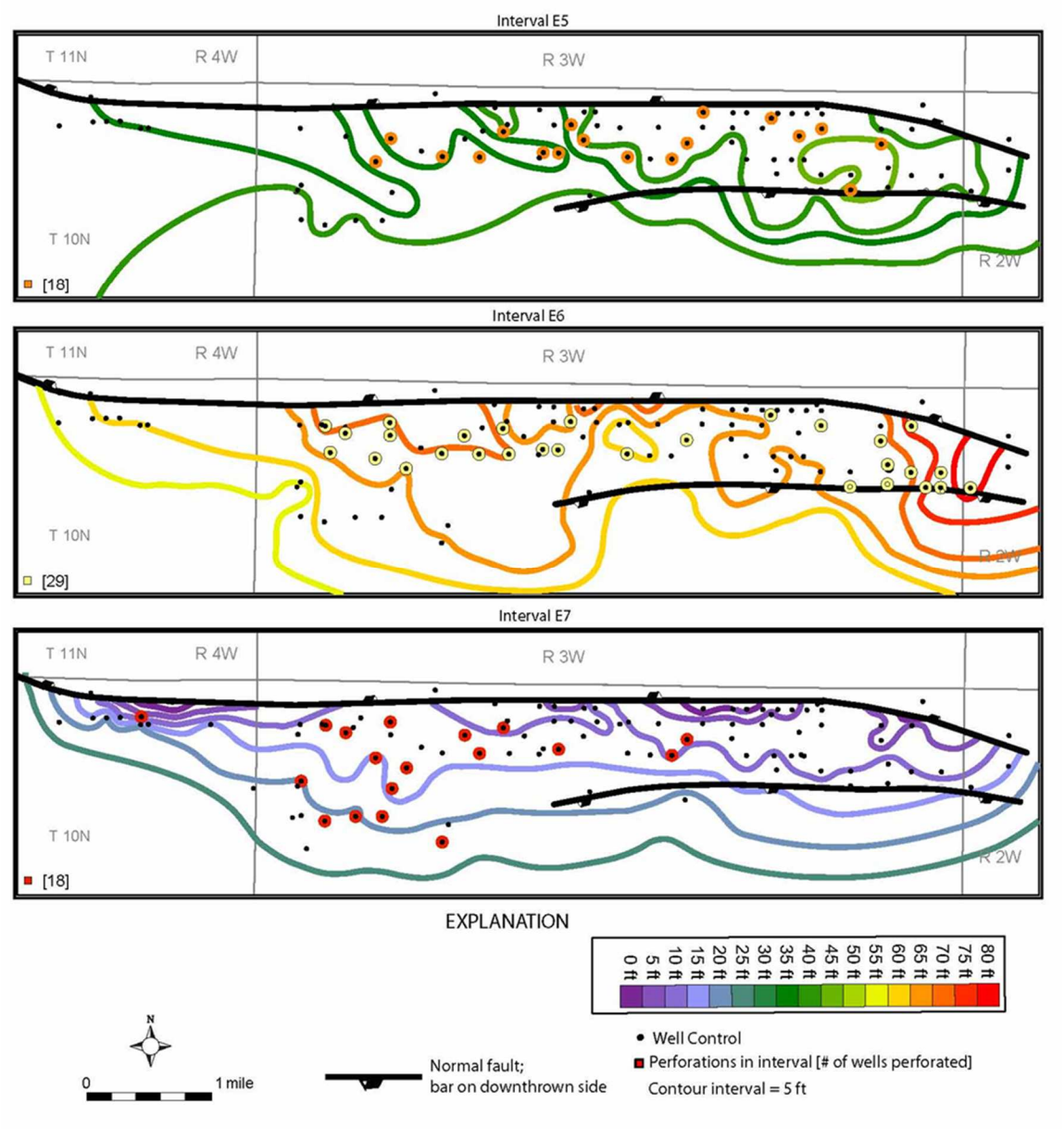

Figure 10. Isopach maps of intervals E5-E7, eastern Gilbertown Field.

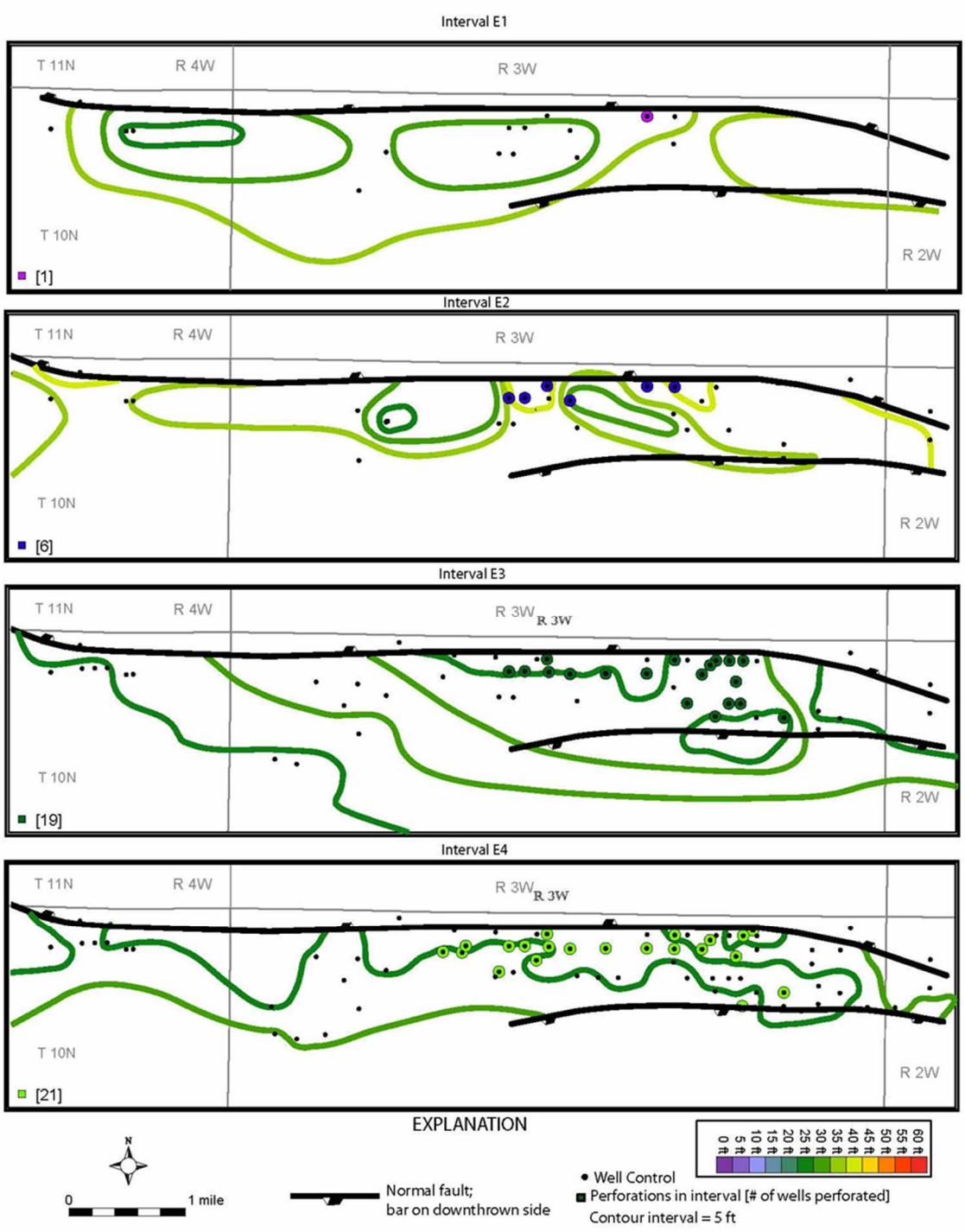

Figure 11. Net sandstone isolith maps of intervals E1-E4, eastern Gilbertown Field.

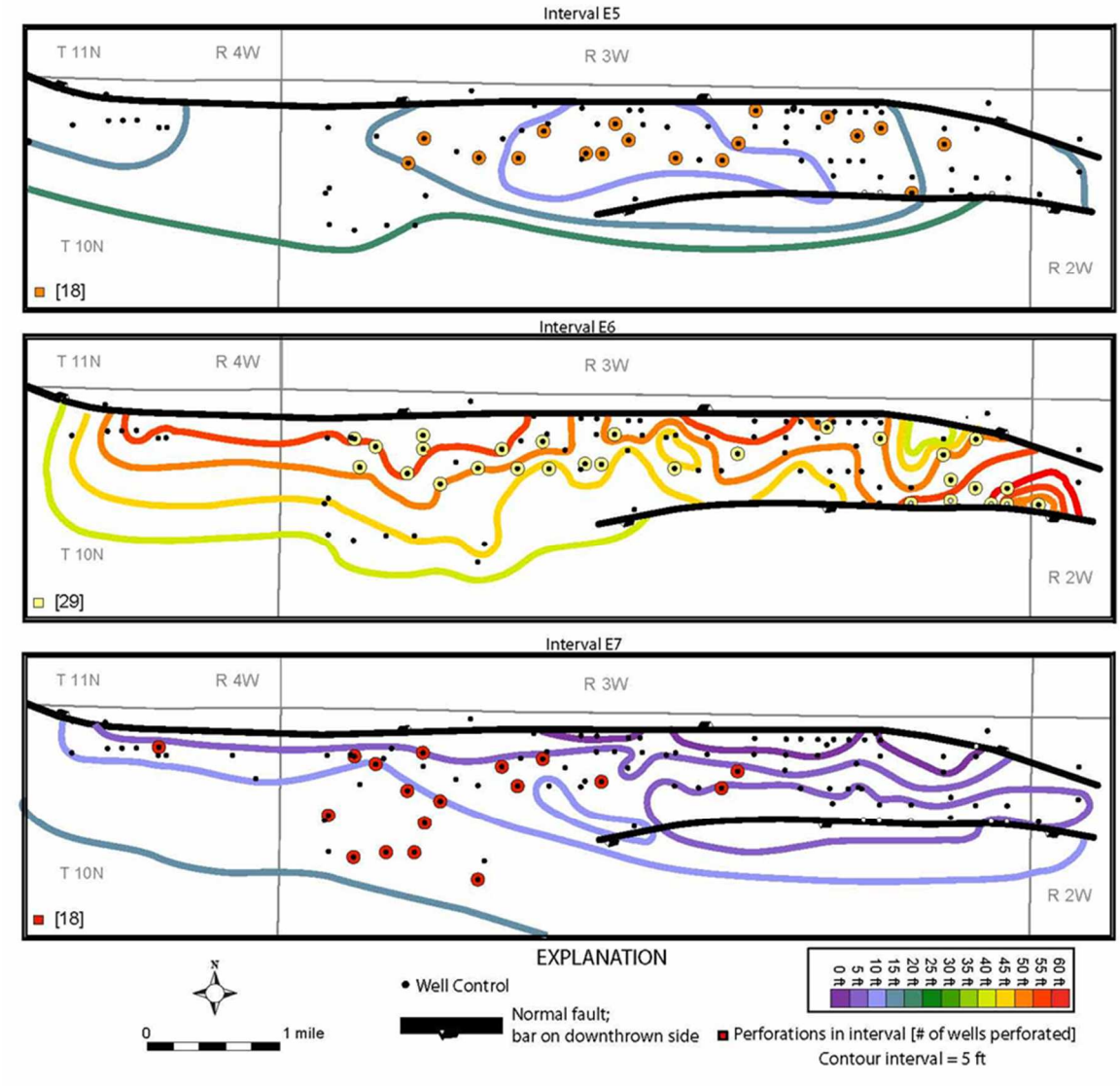

Figure 12. Net sandstone isolith maps of intervals E5-E7, eastern Gilbertown Field.

Petrology

Monocrystalline quartz grains make up the bulk of the primary detrital framework of Eutaw sandstone, typically composing more than 80% of the framework grains, and these grains tend to have strongly undulose extinction (Table 1 and Fig. 14). Based on a single thin section, quartz constitutes 72% of the sandstone in interval E2 (Table 1). Interval E3 contains 82 to 90% quartz, and interval E4 contains 72 to 97% detrital quartz. Quartz content in interval E5 is 88%,

E6 is 82% to 90%, and E7 is 90 to 92% (Table 1). Polycrystalline quartz is a minor framework constituent, ranging from 0 to 5% of the whole rock, and 0 to 8% of the total quartz population (Table 1).

Feldspar grains constitute 0 to 28% of the framework, and types of feldspar include plagioclase, microcline, and orthoclase (Table 1). Sandstone in interval E2 is made up of 25% feldspar, with 80% of that being orthoclase and 20% microcline (Table 1). Interval E3 contains 10 to 14% feldspar and, of that, 78% is orthoclase, 22% is microcline, and only traces of plagioclase (Table 1). Feldspar content in interval E4 is variable, constituting 3 to 28% of the framework, and the majority of the feldspar is orthoclase (Table 1). The wells with lowest feldspar content are in the crestal region of the structure (Table 1, Fig. 13). Intervals E5 through E7 have the lowest percentages of feldspar (0 to 10%), and as in the other zones, the bulk of this is orthoclase and microcline (Table 1).

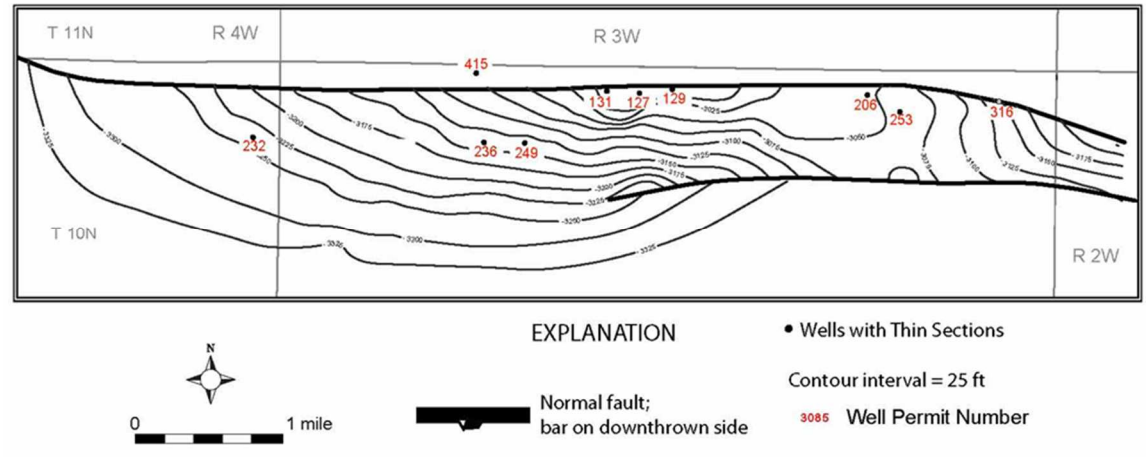

Figure 13. Structural contour map of the Eutaw Formation showing location of wells with thin sections in eastern Gilbertown Field.

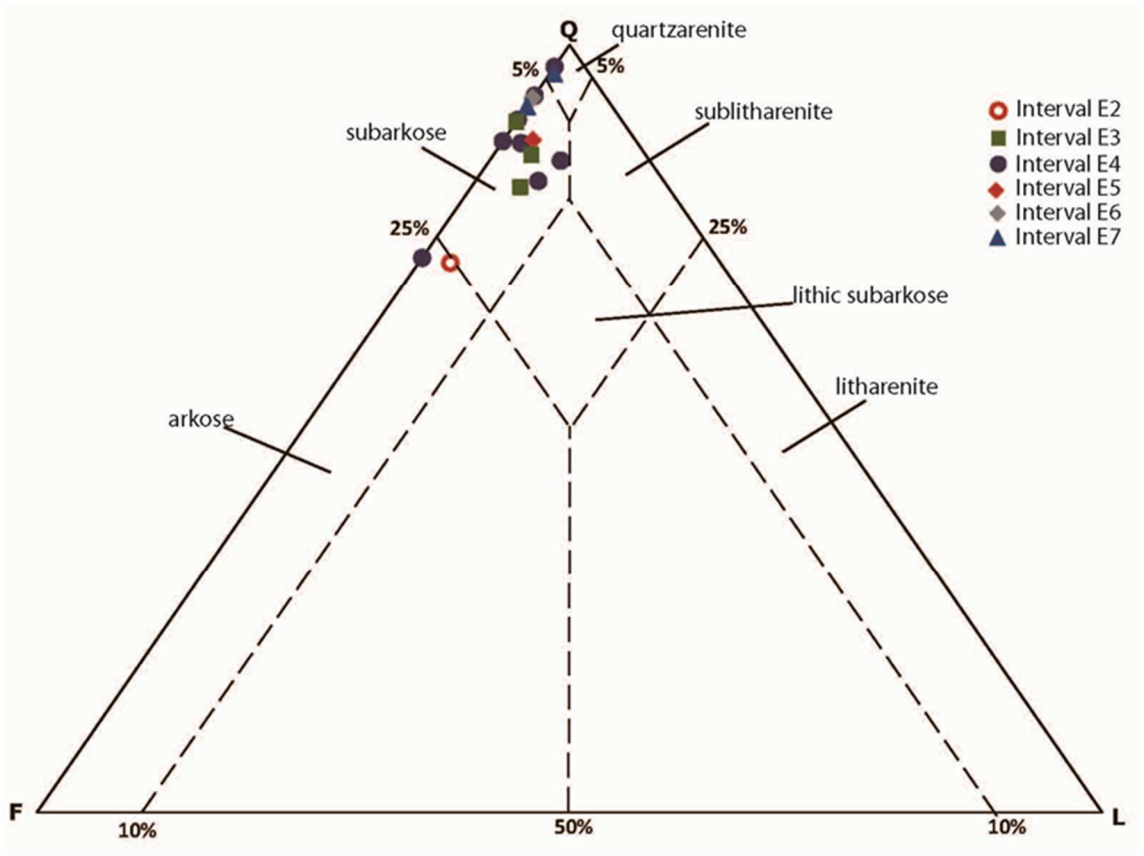

Figure 14. Ternary quartz-feldspar-lithic fragment (QFL) plot showing composition of Eutaw sandstone, eastern Gilbertown Field (sandstone classification from McBride, 1963)

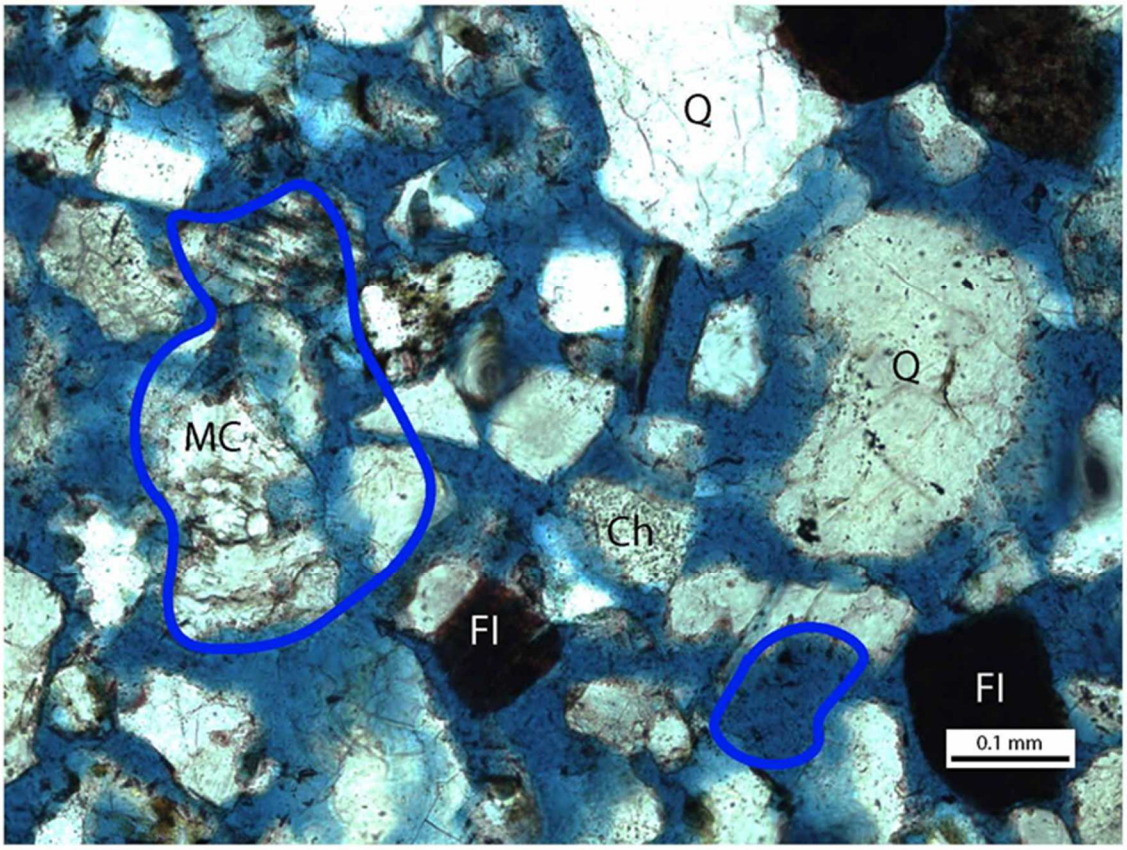

Figure 15. Photomicrograph of subarkosic sandstone from interval E4 (well 316) showing the presence of framework grains, including microcline (MC), chert (Ch), and quartz (Q). Ferric illite (FI) is the dominant authigenic mineral. Blue outlines highlight partially dissolved grains (left) and grain sized molds (lower right).)

Chert and metamorphic rock fragments are the most abundant lithic fragments, with chert being dominant and comprising 0 to 7% of the sandstone and having the classic cryptocrystalline appearance (Table 1, Fig. 15). Metamorphic rock fragments, mainly schistose material, occur only in trace amounts (Table 1). Lithic fragments are most abundant in intervals E4 and E5 but only account for up to 3% of the whole rock (Table 1). Muscovite, zircon, and fossil fragments are other common grain types and can locally constitute up to 10% of the whole rock (Table 1). Muscovite is the most abundant of these and composes 8% of sandstone in interval E4 (Table 1). The muscovite grains are commonly planar and undeformed (Figs. 17, 18).

Using the McBride (1963) sandstone classification, Eutaw sandstone most commonly plots as subarkosic to arkosic (Fig. 14). One thin section from interval E4 and another from E7 plot as quartzarenite (Fig. 14). The sandstone is composed of very fine- to fine-grained sand averaging near 100 µm in diameter. The grains are typically poorly sorted, ranging in size from 60 to > 200 µm but can locally be moderately well sorted (Figs. 15-21). The majority of the grains are angular to subangular and have low sphericity and low to moderate roundness (Figs. 15-21).

Peloidal glauconite can make up as much as 25% of the grains in some of the rocks, and this type of grain is generally characterized as true glauconite (Odom, 1984; Chauduri and other, 1994). This glauconite constitutes 2 to 25% of the sandstone, and sandstone from each interval exhibits a wide range of composition (Table 2). The peloidal glauconite is green, but commonly

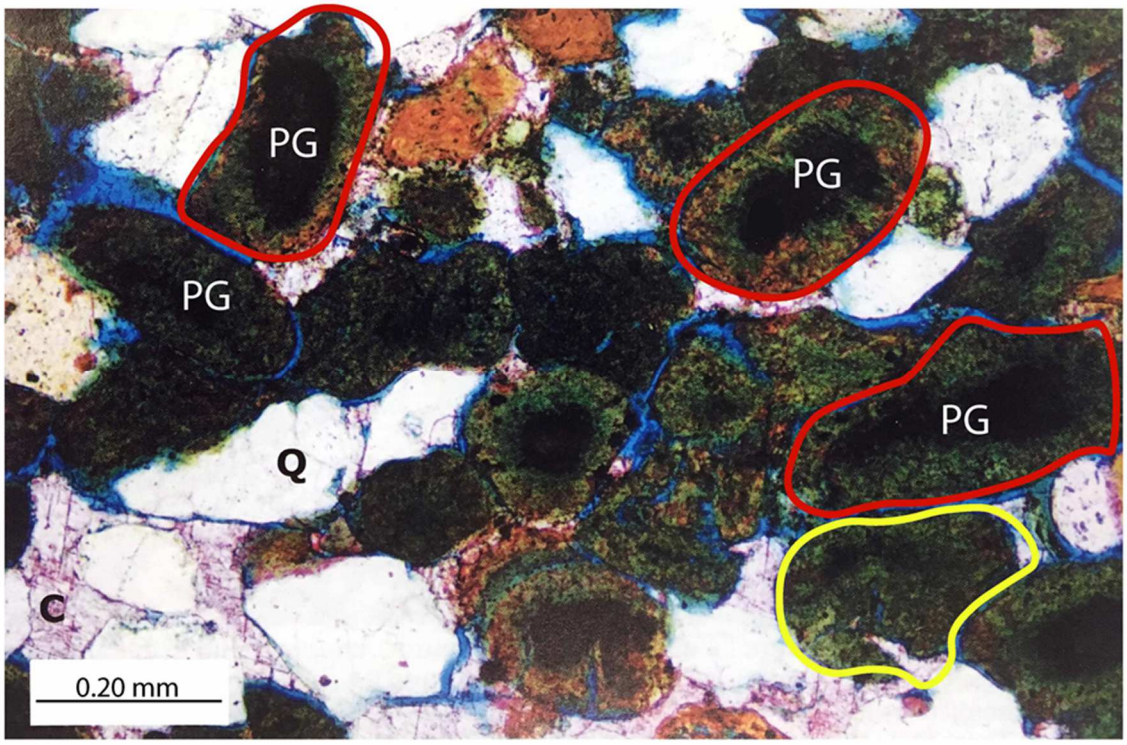

Figure 16. Photomicrograph of subarkosic glauconitic sandstone from interval E3 (permit 131). Red outlines display green peloidal glauconite (PG) with dark centers. Notice the lack of compaction of soft glauconitic grains and angular quartz (Q) grains. Yellow outline marks calcite cement (C) filling fracture in glauconite grain. Also notice porosity rims around glauconite (modified from Pashin et al., 2000).

Detrital Grain Constituents (%)											
Permit / Depth (feet)	Interval #	Quartz	Polyquartz	Plag	Micro	Ortho	Met RF	Chert	Zircon	Muscovite	Fossil Frag
415 / 3,812-3,824	E2	43			2	8		2		trace	
131 / 3,203-3,213	E3	60	3	trace	1	6				trace	
127 / 3,217-3,237	E3	53	trace		1	8		3		trace	
206 / 3,296-3,3313	E3	44	3	trace	2	4	trace		trace	trace	trace
249 / 3,351-3,359	E4	33	1		3	10		trace	2	3	trace
253 / 3,327-3,329	E4	56	1			4		trace		trace	trace
316 / 3,417-3,435	E4	56		trace		8	trace	trace	trace	trace	
206 / 3,276-3,296	E4	42		4		2	trace	3	trace	6	trace
129 / 3,198-3,204	E4	67	2		trace	2		trace	trace	3	
253 / 3,312-3,313.5	E4	48			trace	6		1			
131 / 3,183-3,193	E4	52	1	trace		4				8	
236 / 3,399-3,401	E4	53	3	trace	3	3	trace	2		4	
249 / 3,326-3,329	E5	59	5	2	3	2		2	trace	trace	
206 / 3,177-3,192	E6	51	3			4				trace	trace
316 / 3,315-3,333	E6	38	2		1	2				trace	
232 / 3,429	E7	46	2	2		2		trace	trace	2	5
232 / 3,430	E7	66				3		trace		3	

Table 1. Table showing percentage of detrital grain constituents in each thin section at eastern Gilbertown Field.

appears opaque near the top of the structure due to the absorption of oil (Figs. 16, 17, 18, 21). Brown limonite is also common in the formation. Glauconite makes up 6 to 20% of the sandstone in interval E3 (Table 2). In interval E4, glauconite composes 4 to 24% of the sandstone (Table 2, Fig. 13). Glauconite is least abundant in interval E5, making up just 2% of the sandstone (Table 2). Ferric illite, which is a form of glauconite that is commonly pseudomorphous after albite and mica, occurs in trace amounts throughout the formation and can constitute up to 9% of the sandstone. This type of glauconite also is commonly oil stained but is most commonly dark red to brown and retains the shape and form of the precursor grain (Figs. 15, 19).

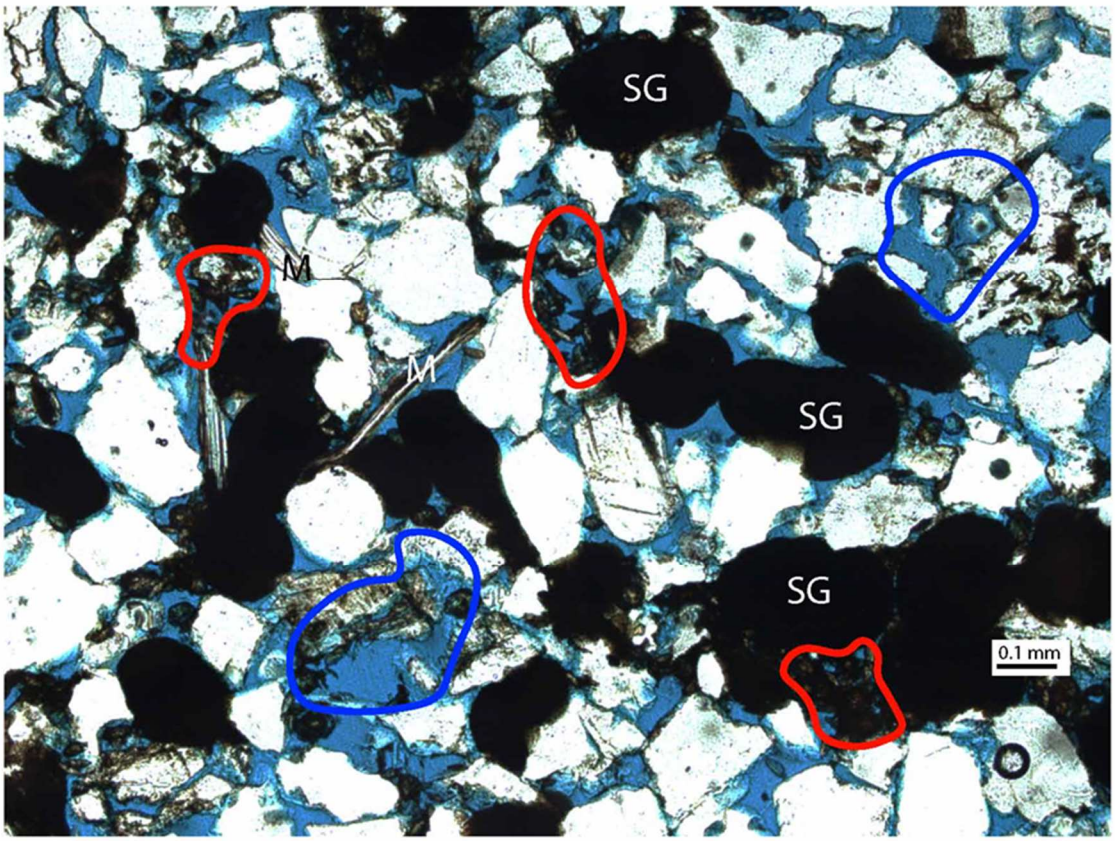

Figure 17. Photomicrograph of subarkosic sandstone from interval E3 in eastern Gilbertown Field (well 206). Red out lines show pore space filled with wheatseed siderite and the blue outlines an example of dissolution of feldspar grains and the mold of a precursor grain. Notice the abundant intergranular primary open pore system (blue background). SG= oil stained glauconite, M=muscovite.

Calcite cement is most abundant in intervals E3 and E6 (Table 2, Figs. 16, 18, 21). It occurs in concretionary patches and occludes porosity. The percentage of calcite cement in interval E3 increases in the wells that are located at the highest part of the structure, where it comprises 21 and 22% of the rock, respectively (Table 2, Fig 16). Both thin sections from interval E6, which are located on the horst, have calcite cement percentages that are high, being 23% in well 206 and 18% in well 316 (Table 2, Figs. 18, 21). Interval E4 has lower percentages ranging from 0 to 5% in well 253 that is located on the horst (Fig. 13). In interval E6, calcite

cement can fill fractures in quartz grains (Fig. 18). Siderite cement occurs as wheatseed crystals and very small rhombohedral shapes; it is present in large patches in some of the thin sections. It occurs in high percentages in intervals E3 and E4 on the horst, where it comprises 9% of the total sandstone in interval E3 and 18% of interval E4 in well 206 (Table 2, Figs. 17, 19, 20). In both intervals, the wheatseed siderite tends to form pore fillings in the sandstone (Figs. 17, 19, 20). Siderite also occurs in trace amounts within interval E6 in wells 206 and 316. Here the siderite is in mainly rhombic form and is a minor pore-filling mineral (Table 2, Fig. 18).

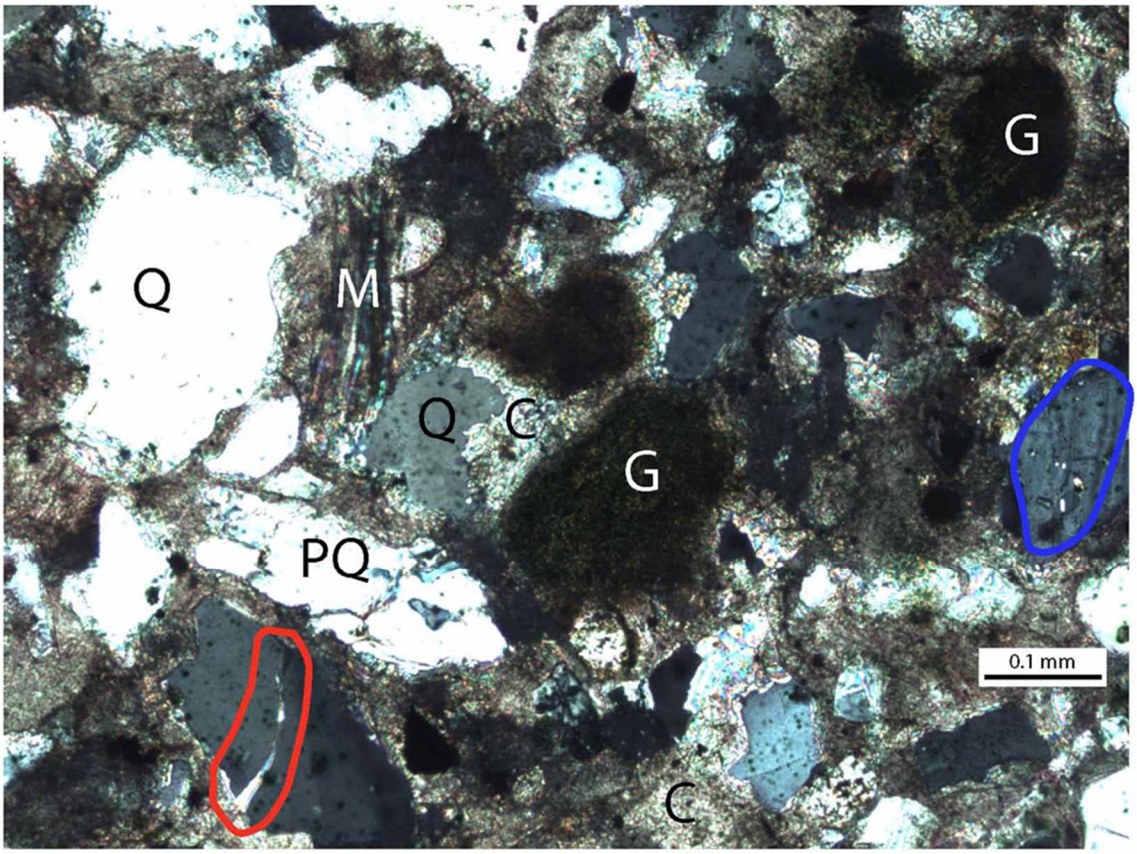

Figure 18. Photomicrograph in XPL of calcite cemented subarkosic sandstone from interval E6 (well 206). Outlined in red is a fractured quartz grain filled with calcite cement and in blue are small rhombohedral siderite crystals. G=glauconite, C=calcite, Q=quartz, PQ=polyquartz, M=muscovite. Notice the lack of pore space and abundance of pore filling calcite cement.

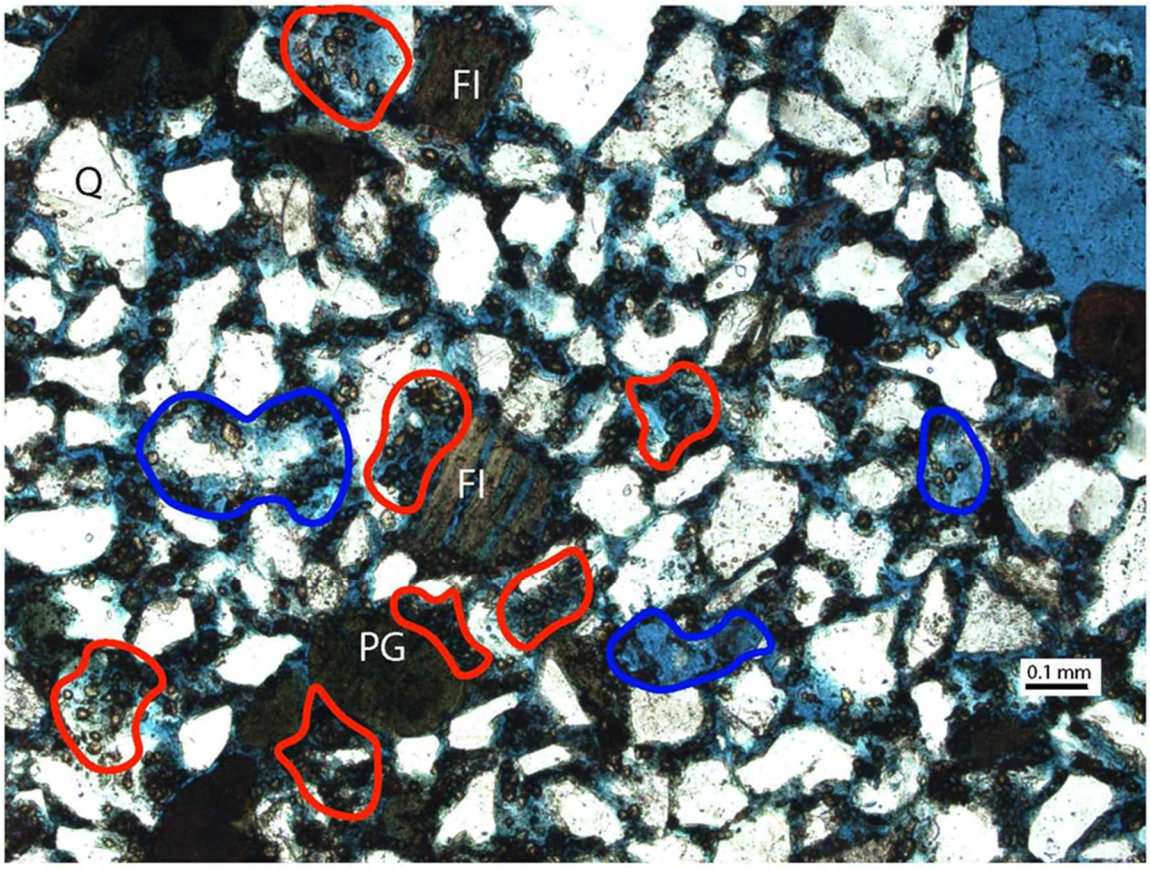

Figure 19. Photomicrograph of subarkosic sandstone in interval E4 (well 206). Angular grains are abundant with low to moderate sphericity. Outlined in red are pores filled with wheatseed siderite, blue outlines mark dissolution pores. Ferric illite (FI) displays intraparticle porosity and peloidal glauconite (PG) is green to brown in color and undeformed.

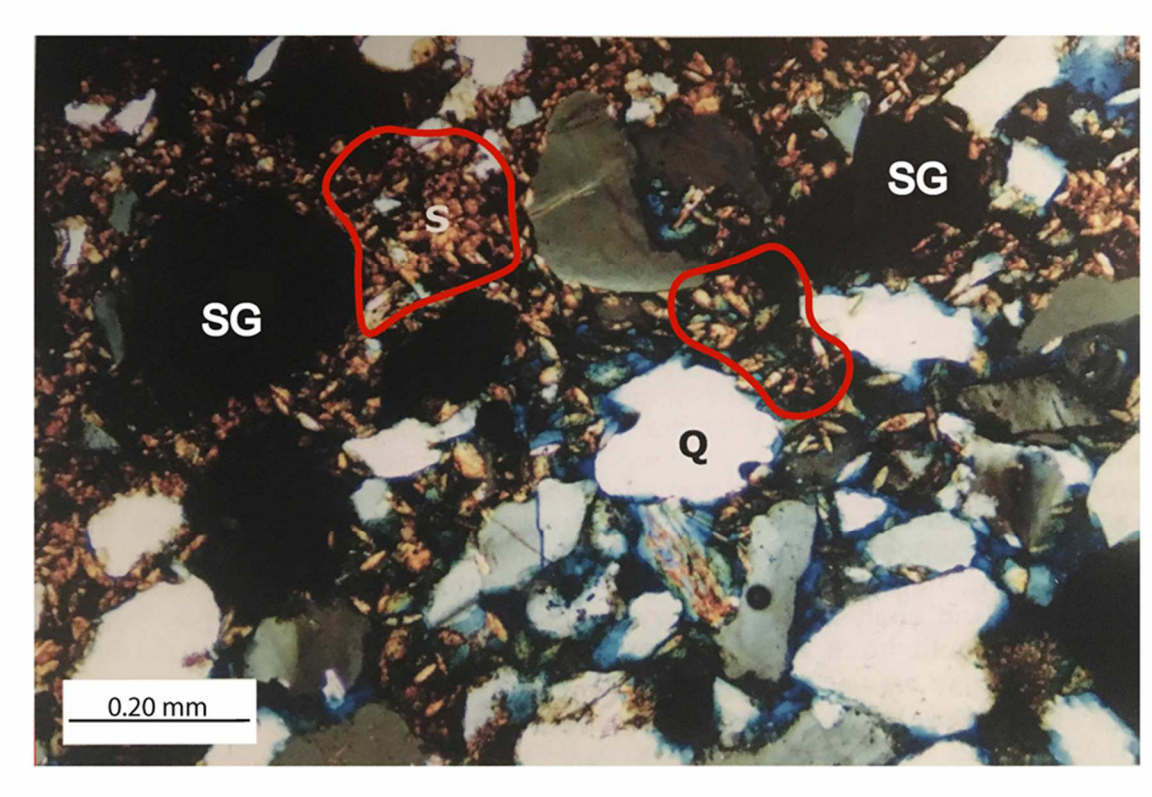

Figure 20. Photomicrograph of subarkosic sandstone of interval E4 (well 206). Glauconite (SG) is stained black with oil and red outlines pore space filled with siderite cement (S). Quartz (Q) grains are angular with low sphericity and roundness (modified from Pashin et al., 2000).

Porosity in the Eutaw Formation is mainly primary interparticle porosity. However, secondary intraparticle porosity is developed throughout the sandstone in vacuolized feldspars. Moldic porosity also is common, as the void sizes are the approximate size of the feldspar grains within the sandstone Figs. 15, 16, 17, 19, 21). Interval E3 has only 1 to 3% porosity in the structurally highest part of the horst, and porosity increases to 18% in well 206, which is in a structurally lower part of the horst (Table 2, Figs. 13, 16, 17). Where calcite cement occludes much of the pore space, rims of porosity surround peloidal glauconite grains (Fig. 16). Porosity is highest in interval E4, ranging from 18 to 25% in most areas and reaching a maximum value of 33% in the central part of the horst (Table 2, Figs.13, 15, 19). The lowest porosity in interval E4 is in well 206, where much of the pore space is filled with siderite; compacted glauconite also occludes porosity (Figs. 19, 20). Interval E5 has an average porosity of 25% with an abundance

of interparticle porosity and little authigenic cement (Table 2). Much like interval E3, interval E6 exhibits heterogeneous carbonate cementation and porosity development. For example, well 206 has an average of only 1% porosity, whereas well 316 has an average of 11% porosity (Figs 13, 18, 21). Interval E7 has average porosity of 15% (Table 2), and as previously mentioned, the sandstone in this interval pinches out in the crestal region of the faulted anticline.

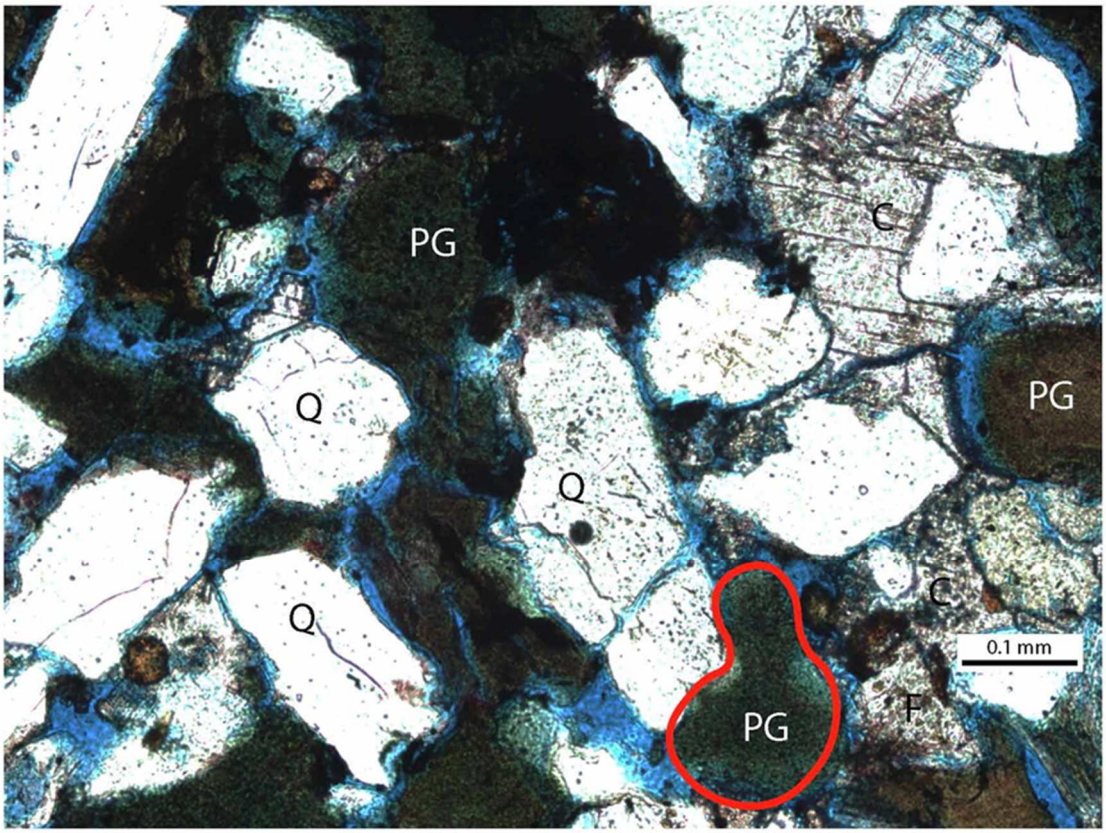

Figure 21. Photomicrograph of subarkosic sandstone of interval E6 (well 316). Glauconite is green and peloidal in habit (PG) and the red outlines a slightly compacted glauconite grain that is filling pore space. Calcite cement is variable and occludes pore space as well. Quartz (Q) grains are angular with low sphericity and roundness.

Diagenetic Constituents and Porosity (%)						
Permit / Depth (feet)	Interval #	Glauconite	Ferric Illite	Siderite	Calcite	Porosity
415 / 3,812-3,824	E2	17	1			27
131 / 3,203-3,213	E3	6	trace		21	3
127 / 3,217-3,237	E3	12	trace		22	1
206 / 3,296-3,3313	E3	20	trace	9		18
249 / 3,351-3,359	E4	24	2		3	19
253 / 3,327-3,329	E4	14	trace		5	20
316 / 3,417-3,435	E4	4	trace			32
206 / 3,276-3,296	E4	18	trace	18		7
129 / 3,198-3,204	E4	15	trace		1	10
253 / 3,312-3,313.5	E4	12	trace			33
131 / 3,183-3,193	E4	15				20
236 / 3,399-3,401	E4	5	4			23
249 / 3,326-3,329	E5	2				25
206 / 3,177-3,192	E6	9	9	trace	23	1
316 / 3,315-3,333	E6	25	3	trace	18	11
232 / 3,429	E7	18				23
232 / 3,430	E7	18	2		1	7

Table 2. Table showing percentage of diagenetic constituents in each thin section of eastern Gilbertown Field.

Log and Core Analysis

The vintage log suite in Gilbertown Field limits the application of the majority of the sandy shale methods described by Asquith (1990), as neutron porosity, density porosity, or sonic logs are required for these procedures. Although the compensation shaly sandstone method of Walsh et al. (1993) and Asquith (1990) requires only SP and resistivity logs to calculate water saturation, applying this method to eastern Gilbertown Field did not yield reliable results. A problem in the Eutaw Formation is that the shallow resistivity used to calculate porosity is much lower than expected in a sandstone with a mud-invaded zone, even for a shaly sandstone. This is the result of conductive minerals, particularly glauconite, ferric illite and siderite, causing false resistivity readings, which in turn makes porosity calculations much too high to be utilized. The effect that the conductive minerals have on the resistivity curves proved to have too great of an impact on resistivity response to yield reliable determinations porosity and water saturation values. Indeed, production of hydrocarbons is common from sandstone with extremely low resistivity (Figs. 7, 8), and correction of resistivity values cannot be accomplished without precise

knowledge of conductive mineral concentration at much higher resolution than the available data allow.

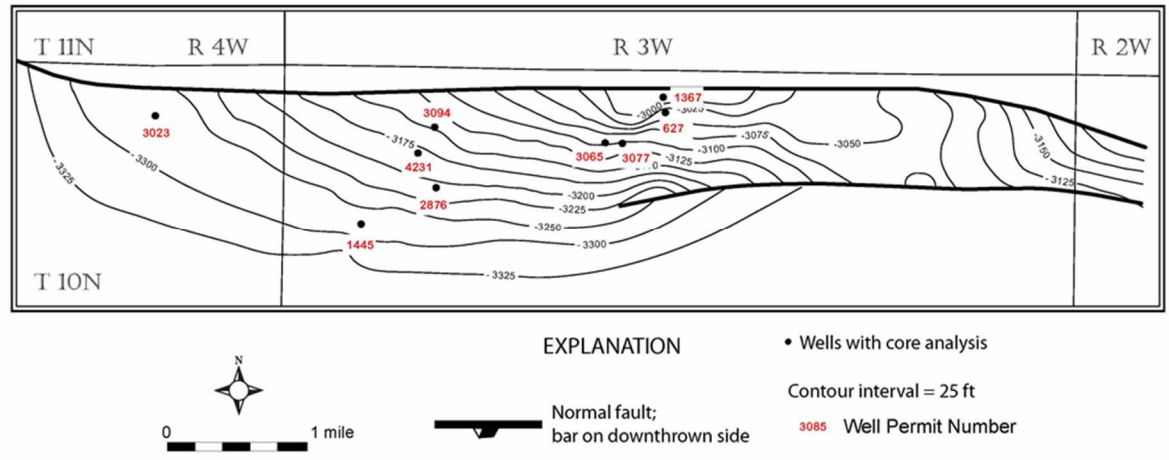

Figure 22. Structural contour map of the top of the Eutaw Formation showing wells with core analysis data, eastern Gilbertown Field.

	n	Log normal mean	Maximum	Minimum	$10^{\sigma-}$	$10^{\sigma+}$	Std. error of log x
All intervals							
Porosity (%)	319	25.5	39.7	12.7	20.6	31.7	0.01
Permeability (md)	308	49.7	5,470.0	0.0	8.5	289.7	0.04
Oil Saturation (%)	185	9.6	38.5	0.0	3.5	26.7	0.03
Interval E7							
Porosity (%)	51	24.0	33.5	15.1	20.1	28.7	0.01
Permeability (md)	42	22.4	540.0	0.0	5.8	86.5	0.09
Oil Saturation (%)	34	5.1	23.2	0.0	2.3	11.4	0.06
Interval E6							
Porosity (%)	56	22.2	33.3	12.7	18.7	26.5	0.01
Permeability (md)	55	16.8	450.0	1.1	5.4	52.1	0.07
Oil Saturation (%)	44	8.0	35.0	0.0	3.1	20.7	0.06
Interval E5							
Porosity (%)	26	24.3	30.6	17.1	20.7	28.6	0.01
Permeability (md)	26	37.7	530.0	2.6	7.4	192.3	0.14
Oil Saturation (%)	17	15.8	30.7	0.0	9.2	27.4	0.06
Interval E4							
Porosity (%)	66	24.3	36.9	16.0	19.9	29.7	0.01
Permeability (md)	66	48.9	2,220.0	2.8	8.5	281.8	0.09
Oil Saturation (%)	32	8.2	38.5	0.0	2.0	34.5	0.11
Interval E3							
Porosity (%)	58	28.7	39.7	15.2	23.0	35.8	0.01
Permeability (md)	57	87.3	5,470.0	3.3	12.3	620.9	0.11
Oil Saturation (%)	25	17.5	31.6	0.0	11.9	25.6	0.03
Interval E2							
Porosity (%)	52	29.6	37.4	16.9	24.7	35.5	0.01
Permeability (md)	52	165.6	1,580.0	5.2	39.9	687.1	0.09
Oil Saturation (%)	26	15.9	35.2	0.0	6.9	36.4	0.07
Interval E1							
Porosity (%)	10	27.1	37.0	19.4	21.9	33.6	0.03
Permeability (md)	10	97.7	1,670.0	6.2	13.9	688.7	0.27
Oil Saturation (%)	10	7.2	37.0	0.0	2.7	19.2	0.16

Table 3. Results of statistical analysis of commercial core-analysis data, Eutaw Formation (Pashin et. al., 200).

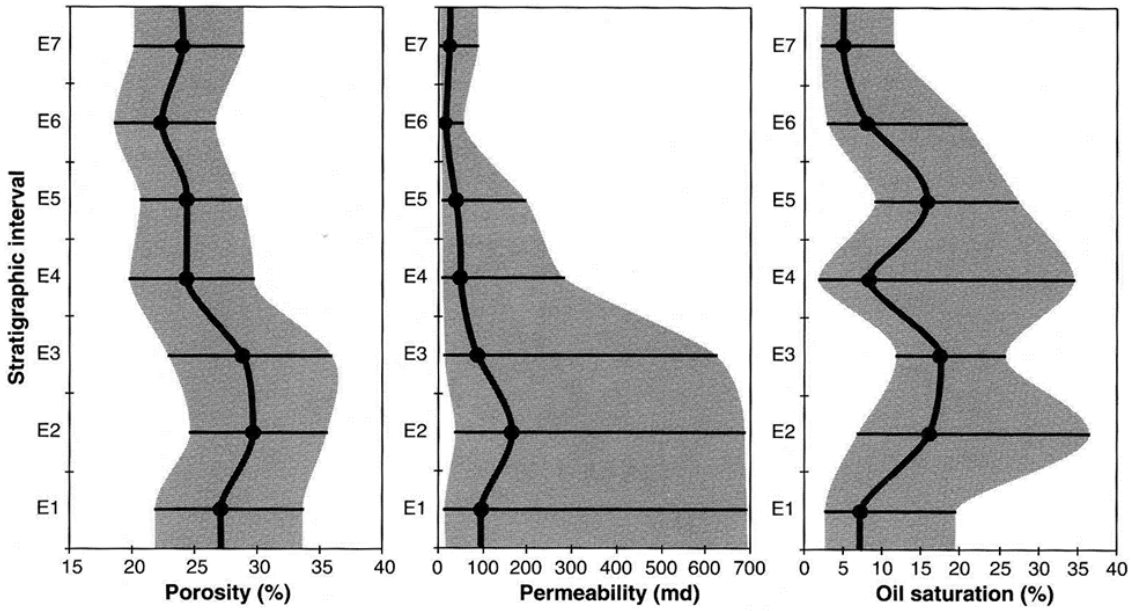

Figure 23. Stratigraphic variation of reservoir quality in the Eutaw Formation, Gilbertown Field. Dark line is the geometric mean, shaded area is lognormal standard deviation (modified from Pashin et al., 2000).

Porosity is commonly high in the Eutaw Formation, having a geometric mean of 25.5%. The maximum value is 39% in interval E3, and the minimum value is 12.7% in interval E6 (Table 3, Fig. 23). Porosity is generally decreases upward in the formation, reaching a minimum in interval E6 with a log normal mean of 22 %. Maps of porosity for each interval are shown in Figures 24 and 25. Porosity trends in intervals E1 through E4 are similar with porosity increasing towards the highest part of the structure (Fig. 24). Porosity patterns in intervals E5 and E7, conversely reflect decreasing porosity related to increasing shale content toward the crest the structure (Fig. 25). Interval E6 has porosity values lower than 20% adjacent to Fault WB, and values increase toward the highest part of the structure adjacent to Fault EGA (Fig. 25).

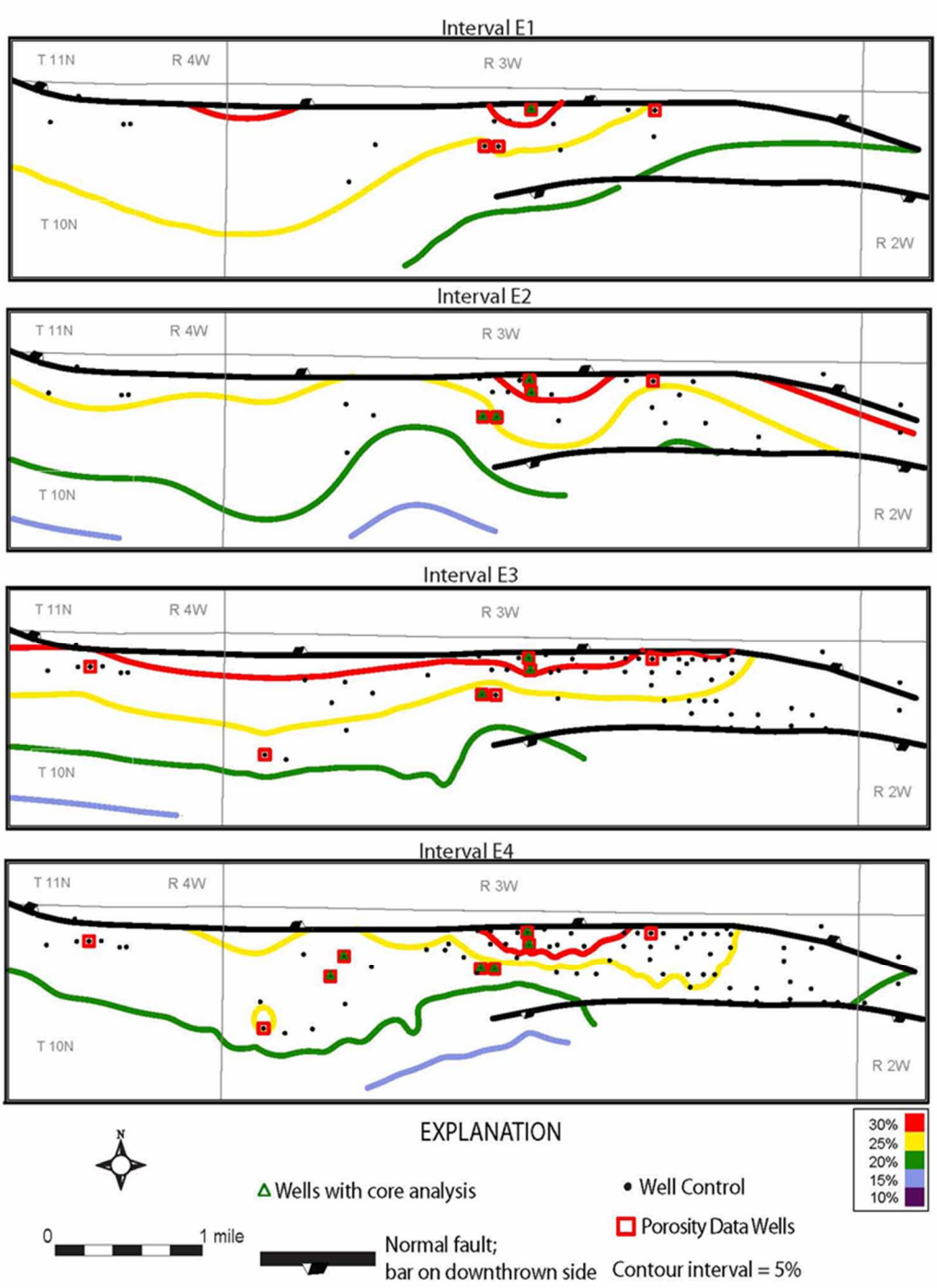

Figure 24. Maps of geometric mean porosity from log and core data in intervals E1-E4, eastern Gilbertown Field.

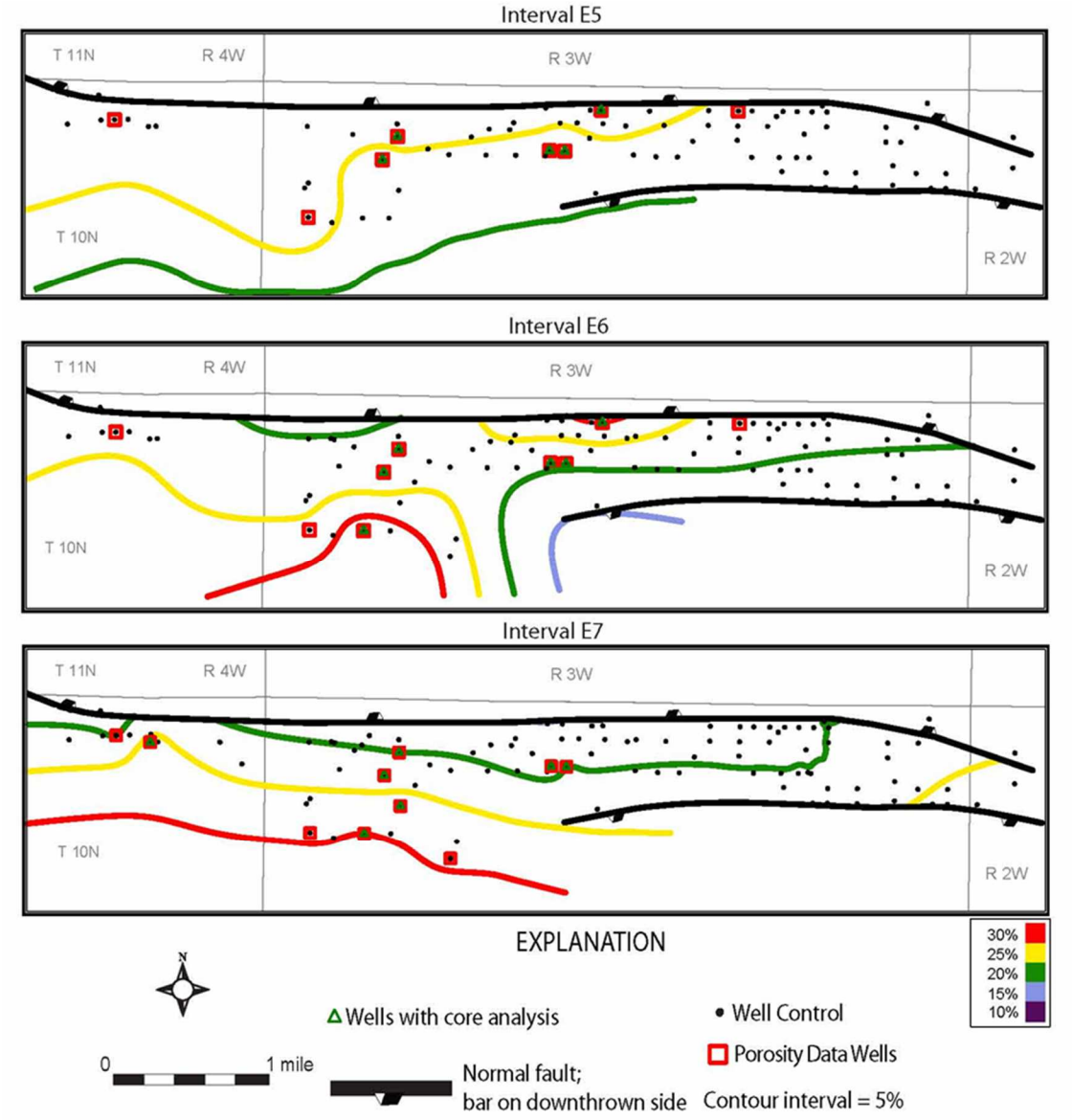

Figure 25. Maps of geometric mean porosity from log and core data in intervals E5-E7, eastern Gilbertown Field.

Permeability varies by orders of magnitude, not only among intervals, but within each given interval (Table 3, Fig. 23). Darcy-class permeability streaks are developed in intervals E1 through E4 with a maximum value of 5.4 Darcies in interval E3. At the other end of the spectrum, values of less than 1 mD are developed in the shaly sections of intervals E6 and E7 (Table 3; Fig. 23). Maps of geometric mean permeability values are shown in Figures 26 and 27. Intervals E1 through E4 have permeability values that increase toward the top of the eastern Gilbertown

structure (Fig. 26). Intervals E5 through E7 have the opposite trend owing to increased clay content and cementation near the crest of the structure (Fig. 27).

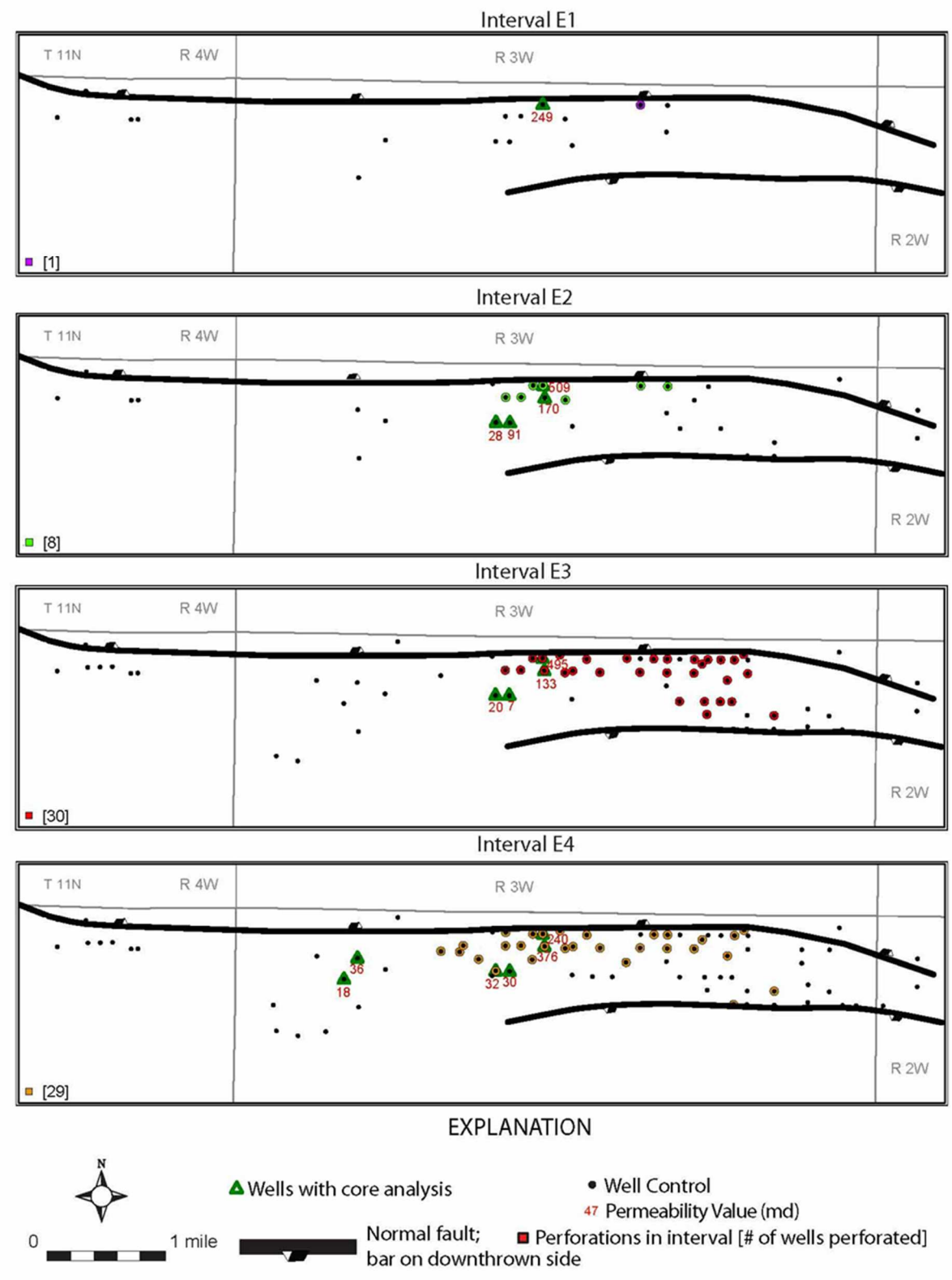

Figure 26. Maps of geometric mean permeability from core data in intervals E1-E4, eastern Gilbertown Field.

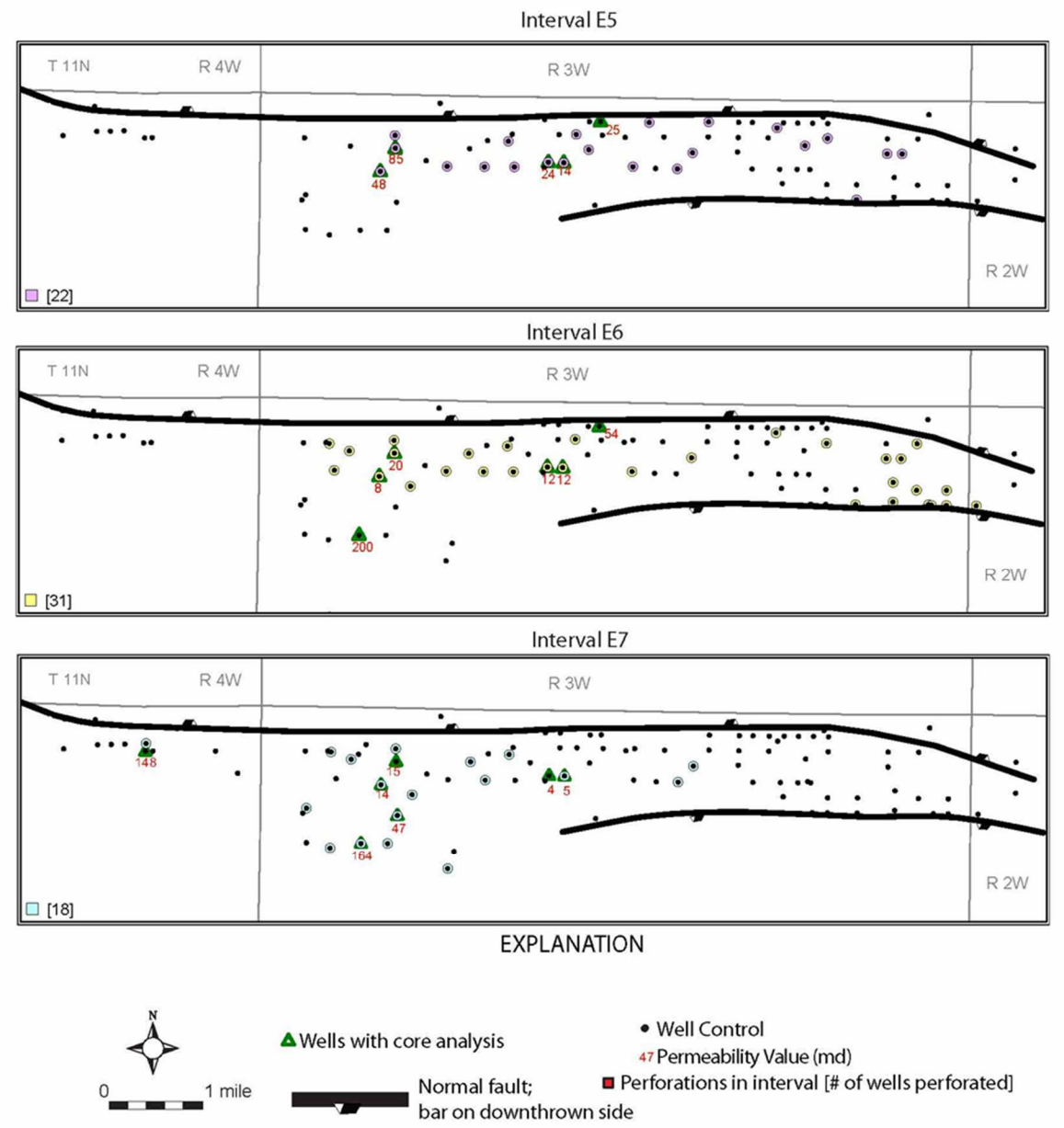

Figure 27. Maps of geometric mean permeability from core data in intervals E5-E7, eastern Gilbertown Field.

Oil saturation is also highly variable, with a maximum value of 38.5% in interval E4 and, importantly, each interval containing sandstone with zero oil (Table 3, Fig. 23). Maps of average oil saturation are shown in Figures 28 and 29. The arithmetic mean of oil saturation in interval E1 is 11% in well 1367 (Figs. 28, 29). Interval E2 has a geometric average of 13% oil saturation from 2 wells that are both high on the structure in the horst (Figs. 22, 27). Interval E3 has a geometric mean of 11% and a range of arithmetic means ranging from 8% in well 627 to 16% in well 1367 higher on the structure (Figs. 22, 27). Interval E4 has a geometric mean of 17%, and ranges from 15 to 20% high on the structure and 14% lower on the structure in well 3065 (Figs. 22, 27). Interval E5 has a geometric mean of 13%, with higher averages in wells on the flank of the structure averaging 14 to 20% and the lowest average is in well 1367 in the highest part of the structure at 5% (Figs. 22, 28). Intervals E6 and E7 have a low average of 7% due to the extreme variation in oil saturation. Although E6 is variable, a general trend is seen and oil saturation increases in the highest part of the structure where it averages 21% in well 1367 (Figs. 22, 28). Interval E7 has low oil saturation on the structure and the highest average percentage in well 323 west of the horst and faulted anticline at 23% (Figs. 22, 28).

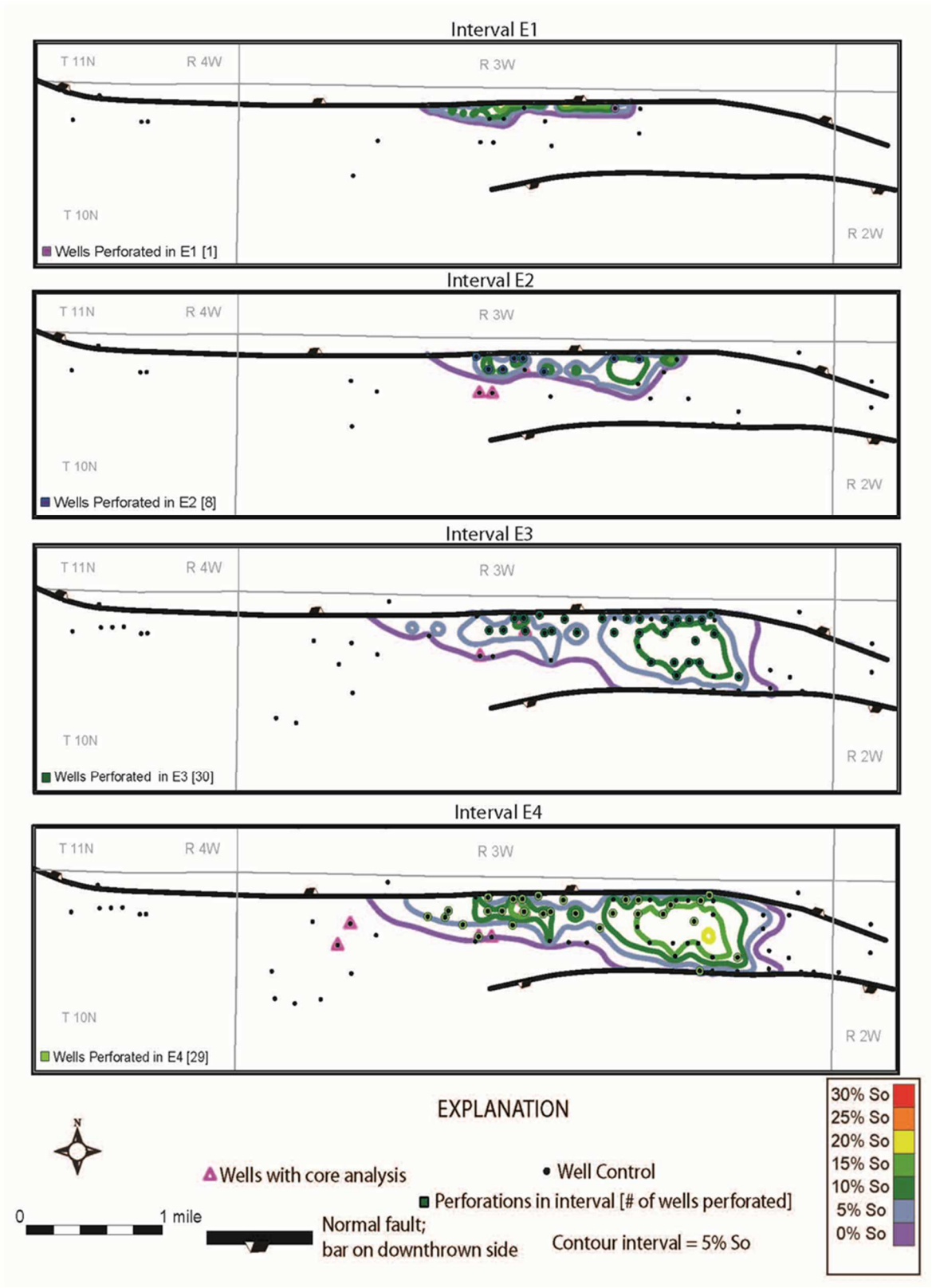

Figure 28. Maps of mean oil saturation in intervals E1-E4, eastern Gilbertown Field.

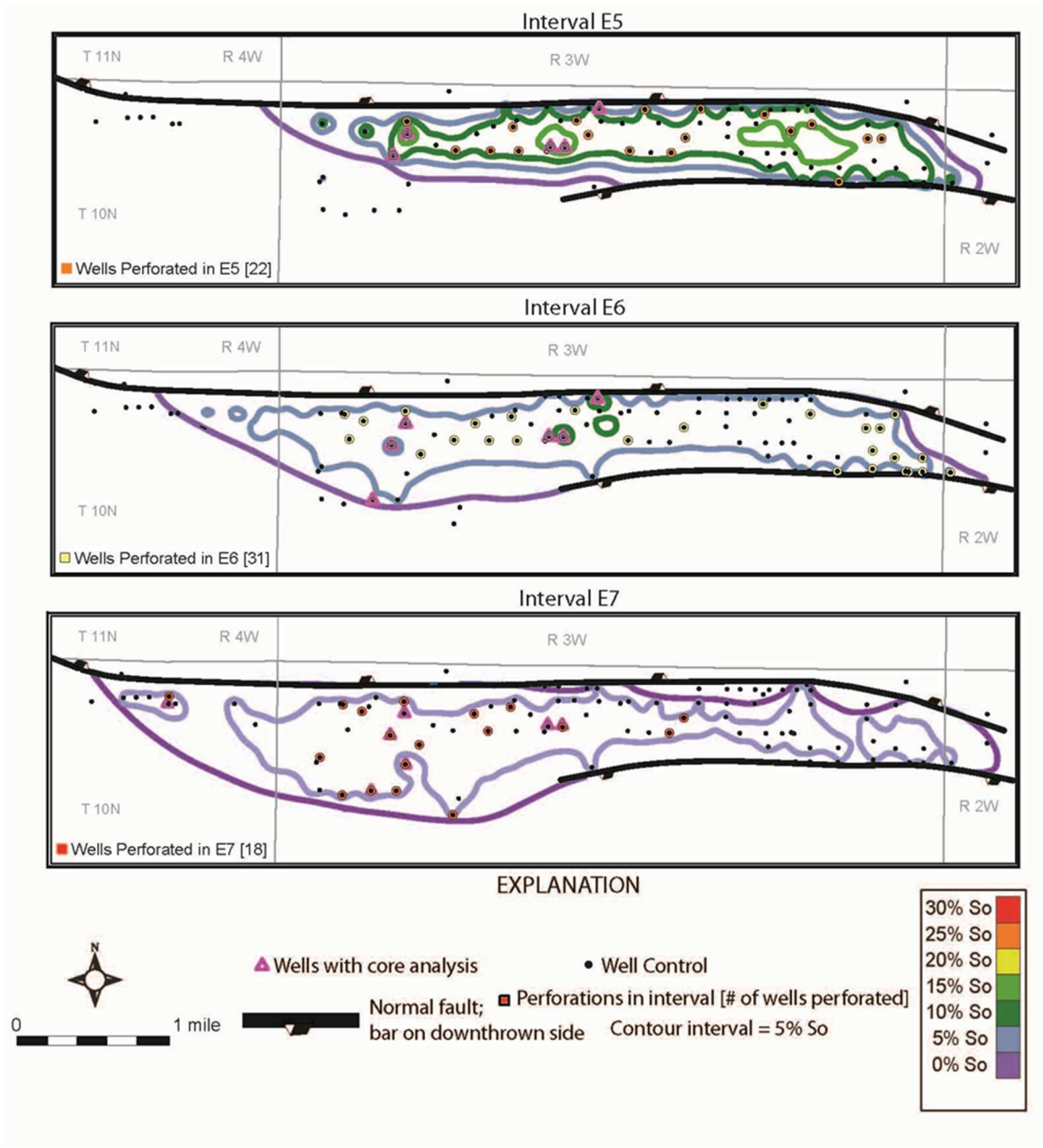

Figure 29. Maps of mean oil saturation in intervals E5-E7, eastern Gilbertown Field.

Water saturation values in the Eutaw Formation are generally high, with geometric means greater than 65% in all of the intervals. Interval E1 has a geometric mean of 83% from well 1367 on the top of the structure, while E2 has a geometric mean of 76%, the highest well on the structure (permit 1367) averages 82% and well 627 has lower Sw averaging 72% (Figs. 22, 30). Interval E3 has a geometric mean of 77% and has slightly lower values high on the structure (Figs. 22 and 30). Interval E4 has a lower water saturation geometric mean of 69%, with the lowest values being in the western part of the horst (Figs. 22, 30). Interval E5 also has a geometric mean water saturation of 69%, with the maximum value being 92% at the top the structure (Figs. 22, 31). Interval E6 has a geometric mean water saturation of 76%, whereas interval E7 has a water saturation average of 75%. Because the oilfield is in such a mature state and the production stream commonly has a water cut exceeding 96% (Pashin et al., 2000), a water saturation cutoff was deemed unnecessary.

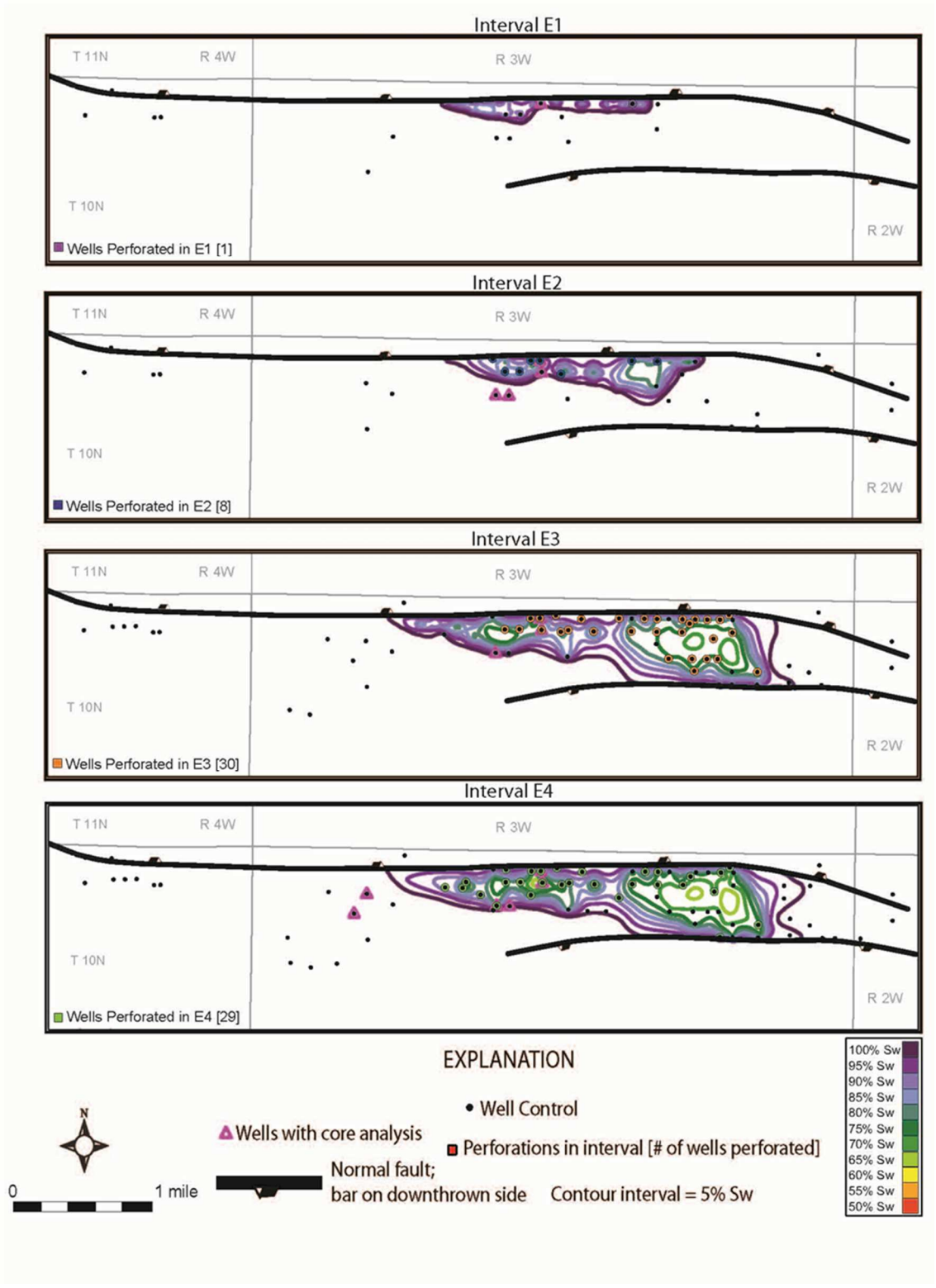

Figure 30. Maps showing mean water saturation in intervals E1-E4, eastern Gilbertown Field.

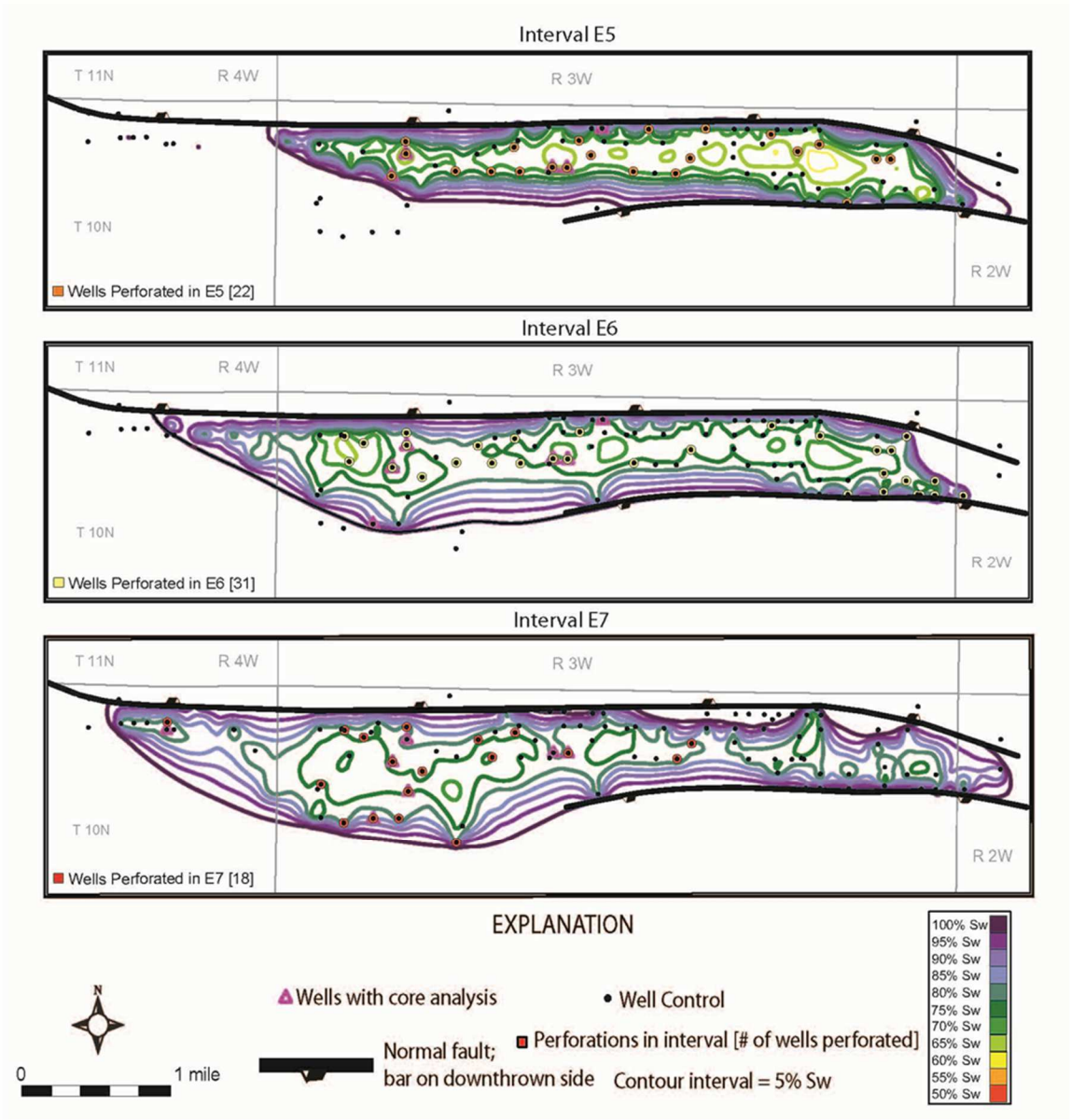

Figure 31. Maps showing mean water saturation of intervals E5-E7, eastern Gilbertown Field.

Volumetric Analysis of Oil-In-Place

SoPhiH ((1-Sw)*porosity*thickness) maps based on the porosity and fluid saturation values discussed above are shown in Figures 32 and 33. Maps showing original oil-in-place (OOIP) per acre for each interval are shown in Figures 34 and 35, and total values of OOIP per interval are in Table 4. SoPhiH values in interval E1 are low due to high water saturation (Fig. 30), and values range from 0 to over 1.5 feet in the structurally highest area of the horst adjacent to Fault EGA (Fig. 32). OOIP values in interval E1 are as high as 10,000 bbls/acre in one small area adjacent to Fault EGA in the structurally highest part of the map area and the interval has a total of 703,000 bbls of OOIP (Table 4). Interval E2 has SoPhiH values ranging from 0 to 2 feet only on the structural high adjacent to Fault EGA, but covers more area of the horst to the south than interval E1 (Fig. 32). Values of OOIP are higher in interval E2 also, exceeding 15,000 bbls/acre in two areas adjacent to Fault EGA. OOIP values in E2 are estimated to be 2.8 MMbbl (Table 4).

The interval E3 reservoir covers much of the horst and contacts both faults. This interval has SoPhiH values higher than 1.5 feet that are abundant throughout the horst and there is an area with values greater than 2 located in the middle of the horst (Fig. 32). Areas in the middle of the horst have OOIP greater than 15,000 bbls/acre, and values greater than 10,000 bbls/acre are common throughout the horst (Fig. 34). Accordingly, OOIP in interval E3 is estimated at 8.2 MMbbl (Table 4). Interval E4 is much like E3 in the extent and distribution of SoPhiH but has SoPhiH values that are typically higher than 1.5 feet (Fig. 32). OOIP values as high as 20,000 bbls/acre are in the structurally highest part of the reservoir, and separate parts of the horst have values greater than 15,000 bbls/acre (Fig. 34). OOIP in Interval E4 is about 9.4 MMbbl (Table 4).

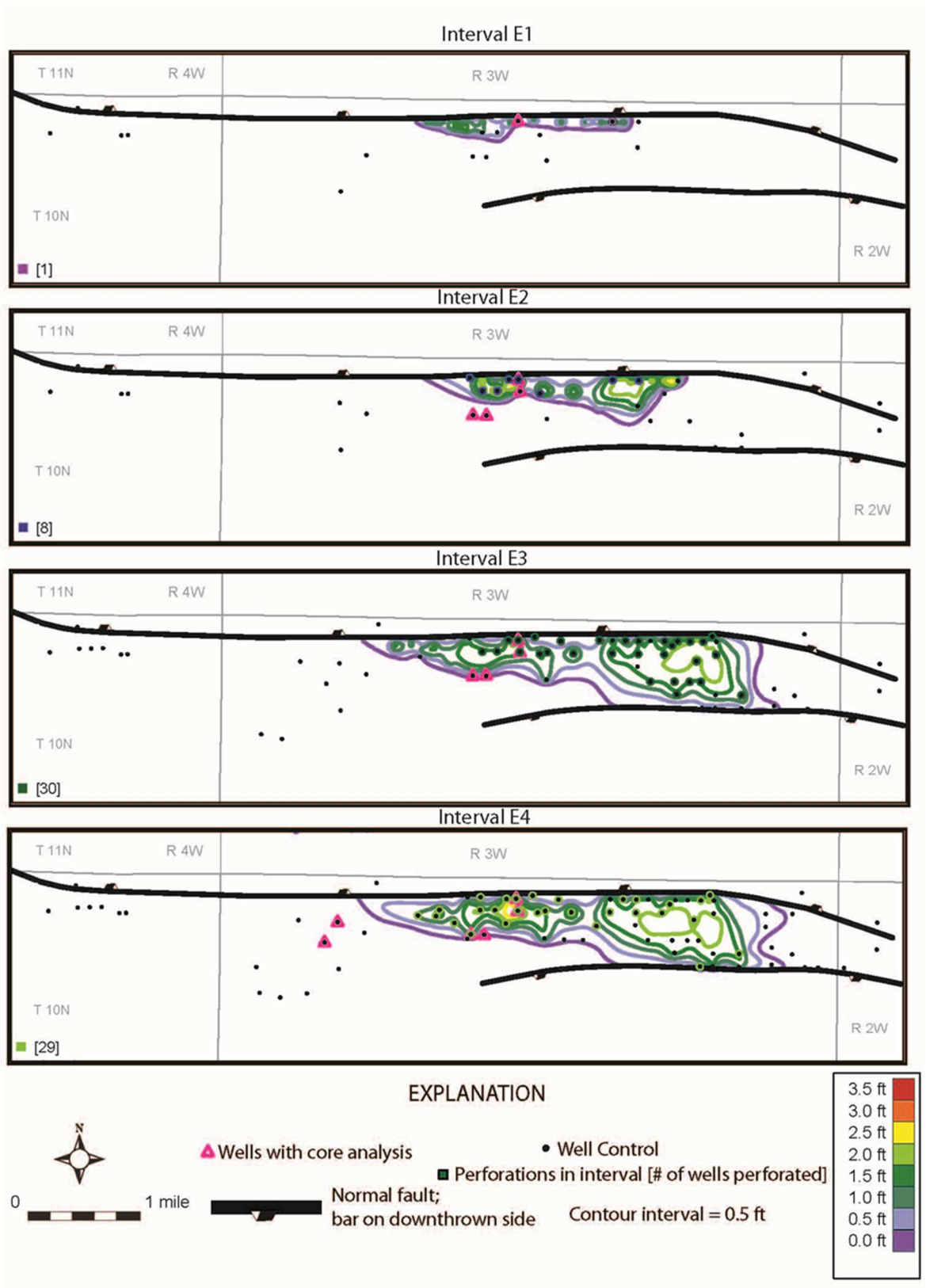

Figure 32. Maps showing SoPhiH (feet) in intervals E1-E4, eastern Gilbertown Field.

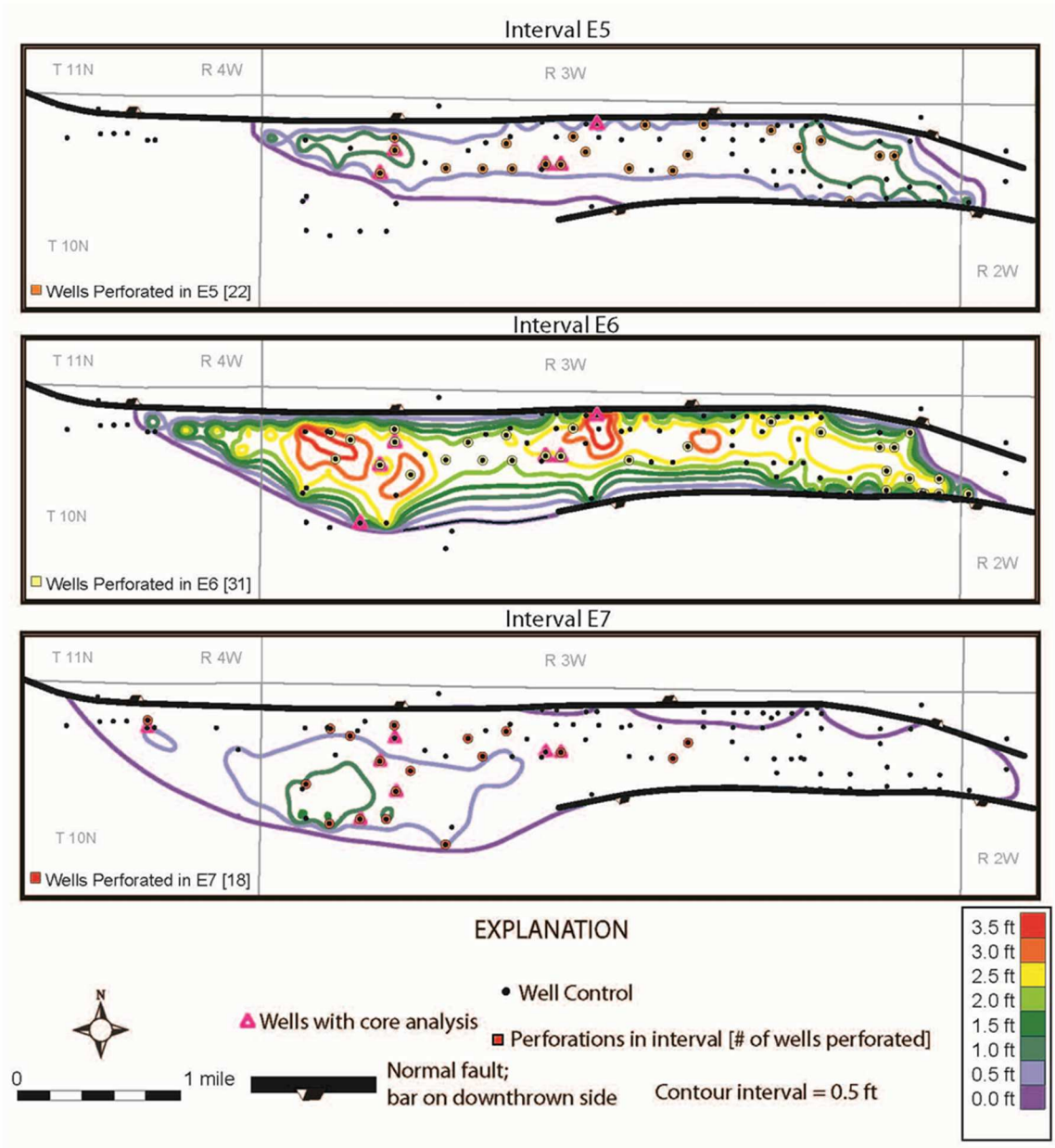

Figure 33. Maps of SoPhiH (feet) in intervals E5-E7, eastern Gilbertown Field.

Interval E5 has lower values of SoPhiH, which only reach 1.5 feet, and the elevated SoPhiH values are in the faulted antlicline west of the horst and in the eastern part of the horst (Fig. 33). Values of OOIP only reach greater than 5,000 bbls/acre, however these values cover the entirety of the central area on the horst and west of the horst on the faulted anticline, and results in 10.4 MMbbl originally in place (Table 4).

Interval E6 has the highest SoPhiH values of all the Eutaw intervals, reaching a maximum value greater than 3.5 feet in two areas. One area is in the structurally highest part of the reservoir adjacent to Fault EGA, and the other is to the west in the faulted anticline (Fig. 33). The high values of SoPhiH in interval E6 reflect high net sandstone thickness values (Fig. 12). Accordingly, interval E6 has the greatest values of OOIP in the Eutaw reservoir, with maximum values greater than 25,000 bbls/acre and values of about 15,000 bbls/acre throughout the vast majority of the horst and faulted anticline. This interval also has the highest OOIP in the Eutaw Formation, which is estimated at 41.6 MMbbl (Table 4).

SoPhiH values in interval E7 are similar to those in E5 in that they are highest off structure (Fig. 33). Values greater than 1.5 feet concentrated in the western portion of the faulted anticline, where the sandstone is thickest (Figs. 12, 33). The values approach zero as the net sandstone pinches out in the structural high adjacent to Fault EGA (Figs. 12, 33). In the western part of the faulted anticline, OOIP values range from 5 to 10,000 bbls/acre; elsewhere OOIP is below 5,000 bbls/acre. Interval E7 has OOIP estimated at 9.3 MMbbl (Table 4).

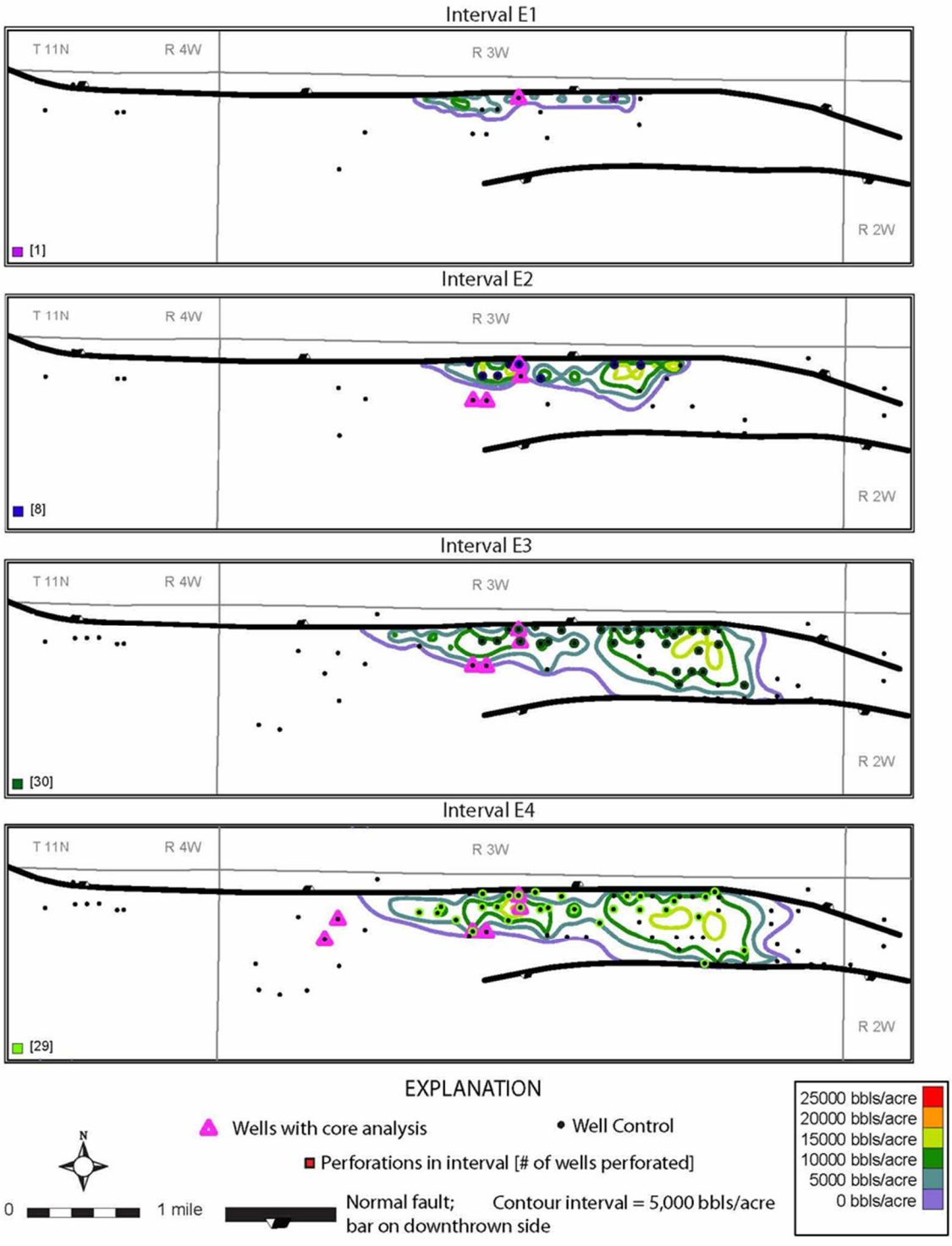

Figure 34. Maps showing original oil-in-place in intervals E1-E4, eastern Gilbertown Field.

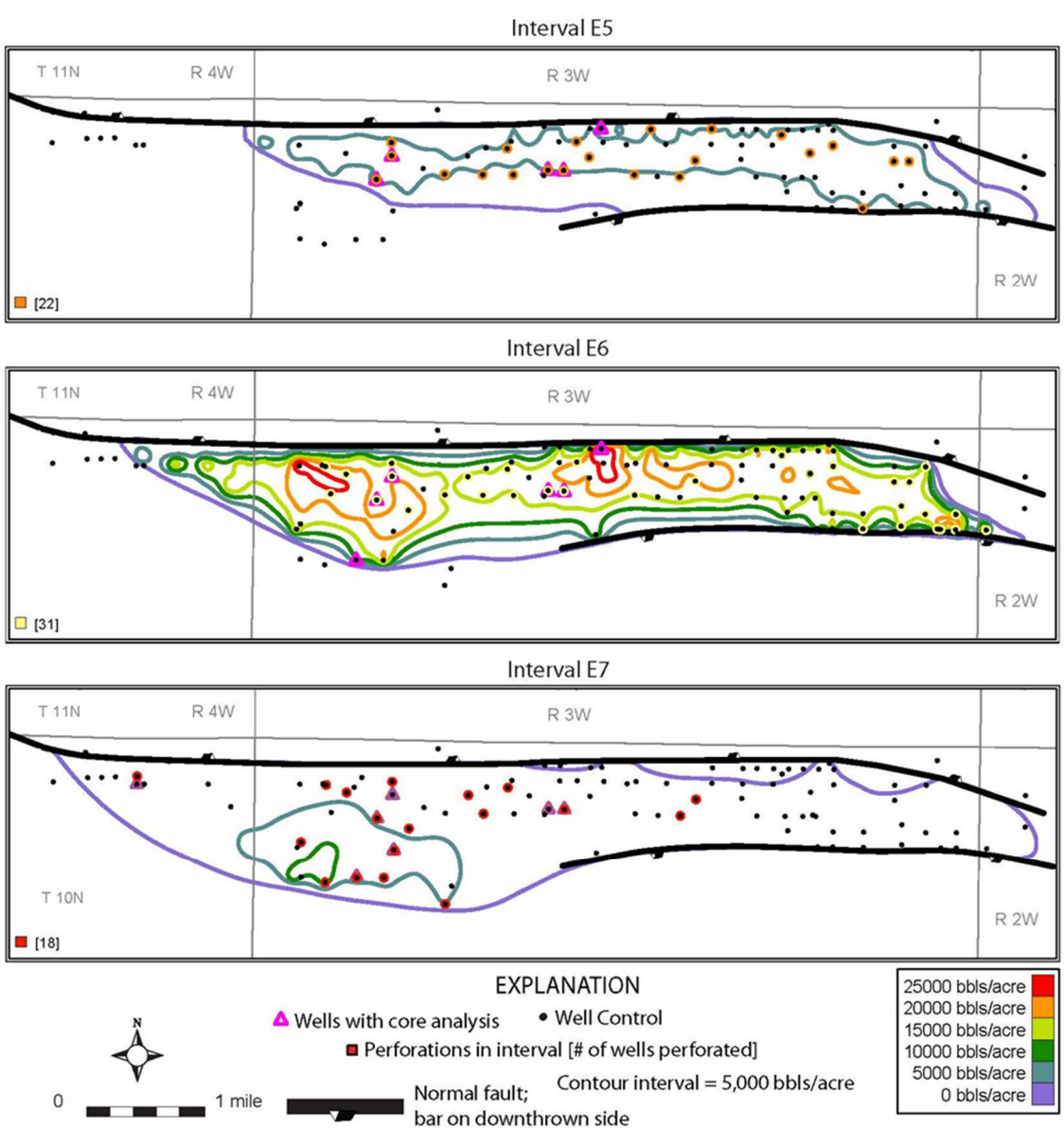

Figure 35. Maps of original oil-in-place in intervals E5-E7, eastern Gilbertown Field.

Figure 36 shows a SoPhiH map that is a summation of all of the Eutaw reservoir intervals. The highest values are in the horst in the structurally highest part of the map area, with values being greater than 10 feet adjacent to Fault EGA. The central and eastern areas of the horst are dominated by values greater than 7 feet, and the lowest values are in the structurally low parts of the map area. OOIP in the Eutaw Formation is calculated to be 82.4 MMbbl (Table 4). OOIP expressed as bbl/acre is shown in Figure 37. The strucuturally highest part of the horst has values greater than 100,000 bbls/acre, and values ranging from 40 to 70,000 bbls/acre are common. The faulted anticline to the west of the horst in places contains than 40,000 bbls/acre.

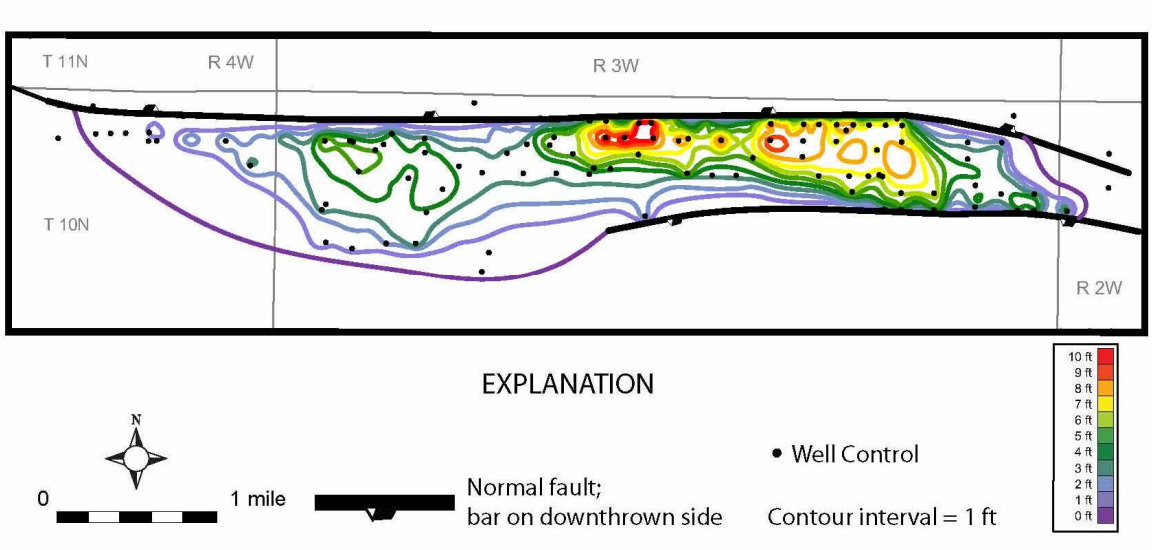

Figure 36. Maps showing combined SoPhiH (feet) in all seven Eutaw Formation intervals, eastern Gilbertown Field.

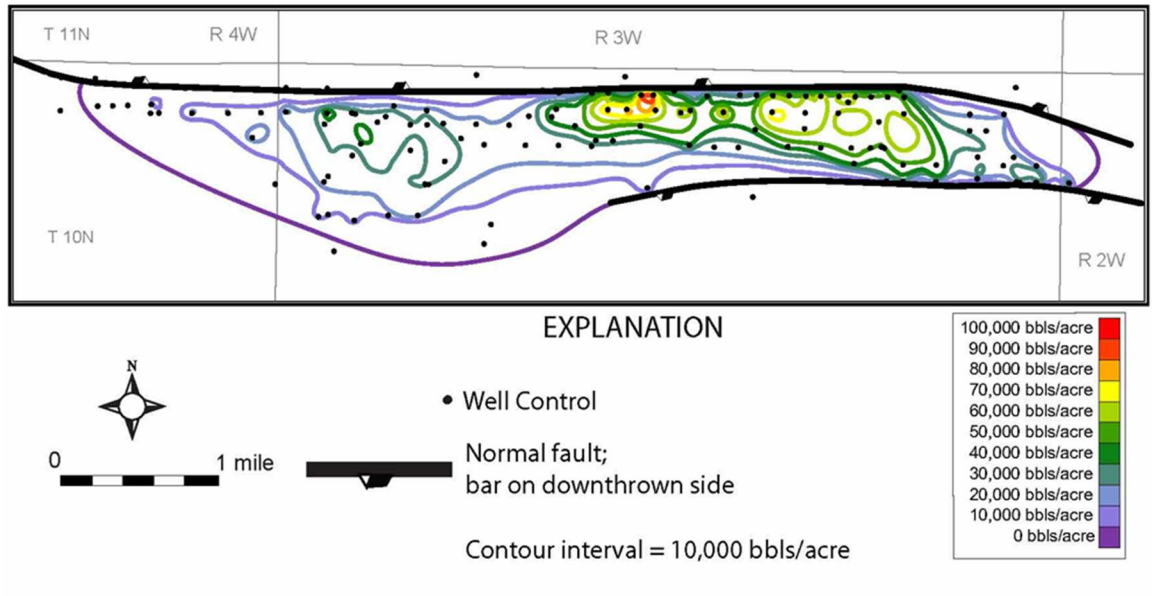

Figure 37. Maps showing combined original oil-in-place values in all seven Eutaw Formation reservoir intervals, eastern Gilbertown Field.

Interval	E1	E2	E3	E4	E5	E6	E7	Total
OOIP (MMbbl)	0.703	2.8	8.2	9.4	10.4	41.6	9.3	82.4
Production (MMbbl)								12
ROIP (MMbbl)								70.4

Table 4. Results of original oil-in-place (OOIP), production analysis (Production), and remaining oil-in-place (ROIP).

Production and Completion Data

Well completion dates in eastern Gilbertown Field are shown in Figure 38. The wells drilled between 1940 and 1950 are primarily adjacent to Fault EGA. From 1950 to 1960, the most wells were drilled (51) and wells ventured further to the east and south. From 1960 to 1990, 51 wells were drilled in the field, mostly infilling between wells, but also testing the southern extension of production near Fault WB and in lower elevations of the faulted anticline.

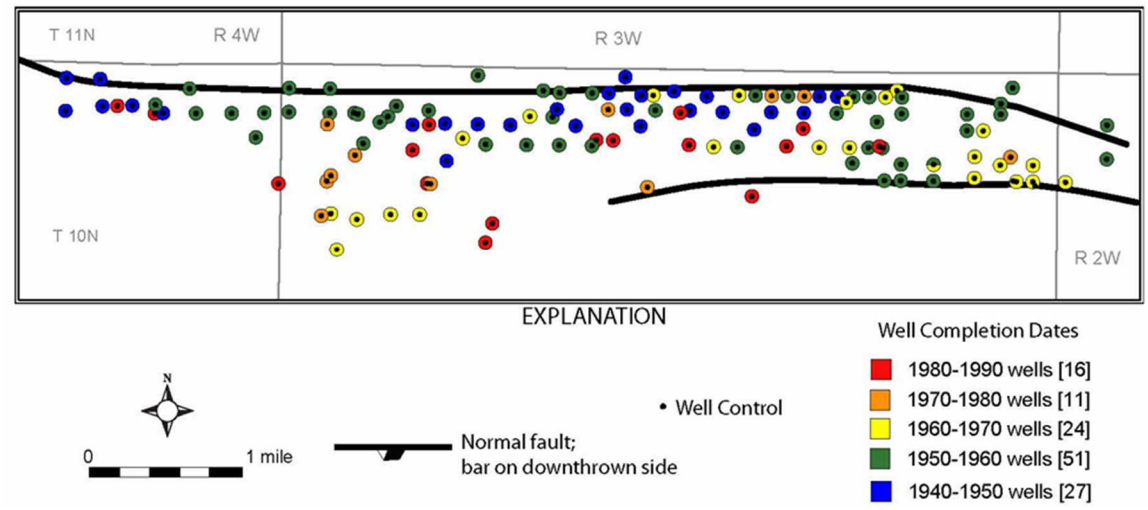

Figure 38. Map of well completion dates, eastern Gilbertown Field.

A map showing perforated intervals and structural contours of the top of the Eutaw Formation is shown in Figure 39. Interval E1 has only produced from 1 well adjacent to Fault EGA, and interval E2 has been perforated in 8 wells, all in the structurally highest part of the horst. In this interval, the lowest known production is at an elevation of -3,230 feet. Production from interval E3 is distributed among 30 wells in the horst, and the lowest known oil in this inteval is at an elevation of -3,250 feet. Interval E4 is much like interval E3 in that production is widespread in the horst. Interval E3 has been completed in 29 wells. Interval E4 has been completed in more wells than E3 in the western side of the horst adjacent to Fault EGA. Also, a large area in the southern part of the horst has not been perforated in interval E4. Interval E4 has lowest known oil at an elevation of -3,225 feet. Interval E5 is mainly perforated in the crestal part of the anticline and in the central part of the horst, with one lone well near Fault WB and another adjacent to Fault EGA, Interval E5 has lowest known oil at an elevation of -3,275 feet. E5 is not as productive in the structurally highest part of the reservoir and most of the area adjacent to Fault EGA, apparently because of high shale content.

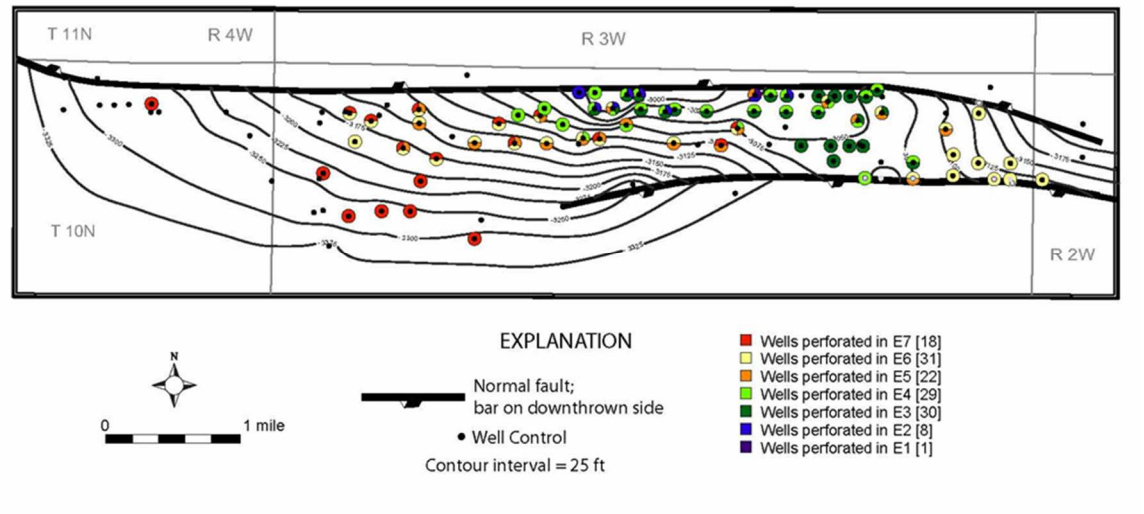

Figure 39. Structural contour map of the top of the Eutaw Formation showing wells with zones perforated in each Eutaw interval, eastern Gilbertown Field.

In all, Interval E5 was perforated in 22 wells. Interval E6 is completed primarily in the flanks of the faulted anticline and has produced from 31 wells. The lowest known oil production is from -3,275 feet. Production from interval E7 is predominantly in the western part of the map area in the flank of the faulted anticline and, to a lesser extent, in the horst. The deepest perforations are at an elevation of -3,300 feet, and E7 has been perforated in 18 wells.

Approximately 12 million barrels of oil were produced from 1945 to 2016 in the Eutaw Formation in eastern Gilbertown field. Cumulative oil production is shown in a production bubble map (Fig. 40). Analyzing cumulative production alone can be somewhat misleading because production is comingled among different Eutaw sandstone intervals. In general, high production values increase with the number of intervals perforated. The five wells with production greater than 600,000 bbl are high on the structure, where most sandstone intervals are productive. Six wells have produced 300,000 to 600,000 bbl. These wells are primarily scattered in the horst. Eleven wells have produced 150,000 to 300,000 bbl; production at this level is widespread, and some of these wells were completed in only one interval. Forty of the wells in eastern Gilbertown Field have produced 200 to 150,000 bbls of oil. Some of these wells

produced for only a short amount of time and were shut in, presumably because of underperformance.

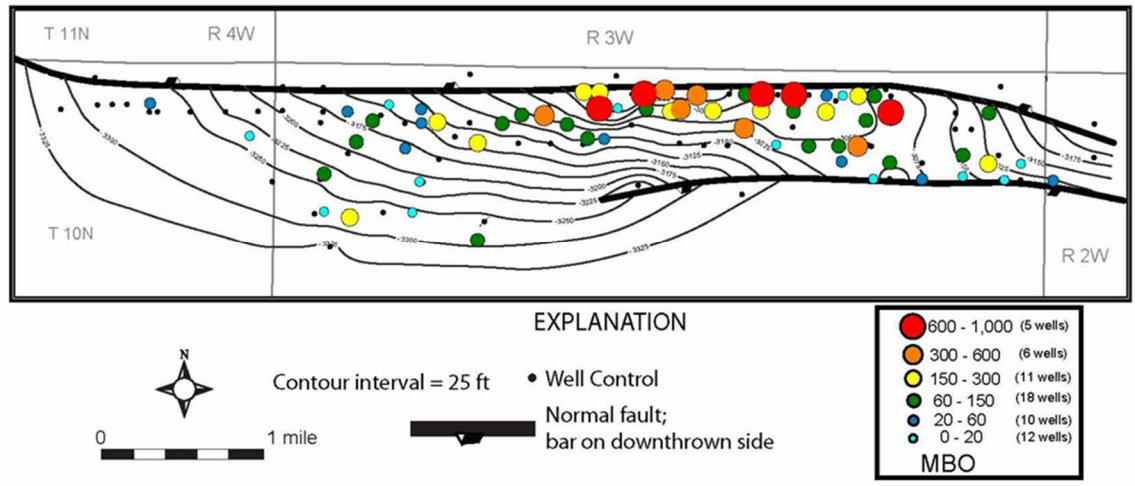

Figure 40. Structural contour map of the top of the Eutaw Formation showing cumulative oil production from the Eutaw Formation, eastern Gilbertown Field.

Two areas in eastern Gilbertown Field have been unitized for waterflooding (Fig. 41). The East Gilbertown Unit is in the southeast portion of the map area, and wells in the unit have been completed primarily in interval E6 (Figs. 39, 41). The unit was established on December 1, 1974, and the last production was reported April 1, 1998. The unit produced 184,275 bbls of oil and averaged 600 bbl of oil per month, with the maximum being 1,619 bbls of oil in November 1976. The Gilbertown (Eutaw Sand) Unit is in the structurally highest part of the reservoir and contains wells completed primarily in intervals E2, E3, and E4 (Figs. 39, 41). The unit first began producing in April 1996, and the last reported production was in June of 2016. The Gilbertown (Eutaw Sand) Unit has produced 325,454 bbls of oil and averaged 1,379 bbls of oil per month. Maximum monthly production was 3,169 bbls of oil in May 1998.

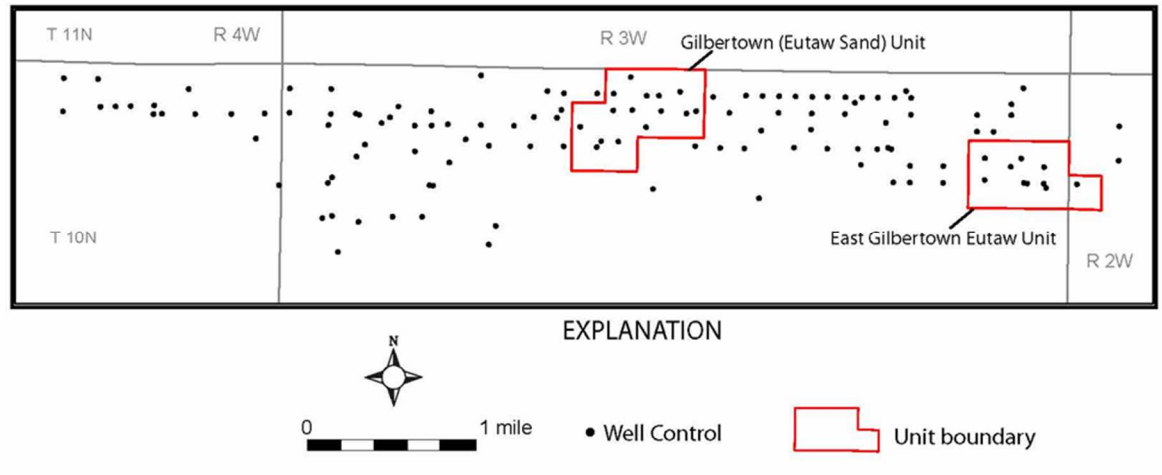

Figure 41. Map of eastern Gilbertown Field showing unitized areas where waterflooding occurred.

CHAPTER V

DISCUSSION

This section synthesizes the results into a cohesive interpretation of the Eutaw reservoir in eastern Gilbertown Field and provides insight into possibilities for future development. Integrating stratigraphic and petrologic analysis provides insight on the depostional setting of the Eutaw Formation. The basal contact of the shale beds of each interval are interpreted as marine flooding surfaces, and hence each interval is considered a parasequence. The presence of coarsening-upward, fining-upward, and serrate log signatures indicates that modes of deposition varied among the intervals. Specifically, the fining-upward to serrate signatures observed in most intervals indicate aggradation, whereas coarsening-upward signatures indicate progradation. All previous workers have interpreted the Eutaw to contain shelf and shore zone deposits (e.g. Cook, 1993; Greer, 1995; Pashin et al., 2000), although supporting data is limited and it is difficult to assign specific environments to each interval.

Thin section analysis reveals that glauconite is present in all of the intervals, and at percentages that clearly affect the resistivity of the Eutaw Formation. Diagenesis of fecal pellets into glauconite occurred very early in marine environments near the sediment-water interface (Cloud, 1955; Odin and Matter, 1981; Velde, 1985) (Fig. 42). The central pellet of the glauconite has not undergone major diagenesis. This type of glauconite is thought to form in situ (Odin and Matter, 1981; Amorosi and Centineo, 1997).

Dissolution of feldspar occurred early and could have contributed to the formation of ferric illite (Fig. 42). Diagenesis of feldspar, mica, pyroxene, and other chemically complex silicate minerals contributes to the formation of ferric illite (e.g. Takahashi, 1939; Galliher, 1935; Light, 1952; Bailey and Atherton, 1969), and so the original sand composition may have been less mature than what was preserved. The presence of ferric illite and peloidal glauconite could be a result of mixing of fresh and saline water during deposition and early diagenesis (Dasgupta et al., 1990; Chaudhuri et al., 1994).

Carbonate cementation is thought to have occurred early in the regional burial history because of the lack of deformation of soft grains like glauconite and muscovite. Siderite cement likely precipitated sometime after the grain dissolution occurred, as the siderite tends to fill large voids that could be molds of grains (Fig. 42). Cement-stratigraphic relationships indicate that calcite cement likely formed after siderite. Pashin et. al., (2000) also noted isopachous grain coatings formed by aragonite. Even where there is an open pore system, the mica and glauconite are undeformed and there is no evidence of quartz overgrowth or contact dissolution, indicating little mechanical compaction of the sandstone. Hydrocarbon migration occurred after diagenesis and may have arrested cementation.

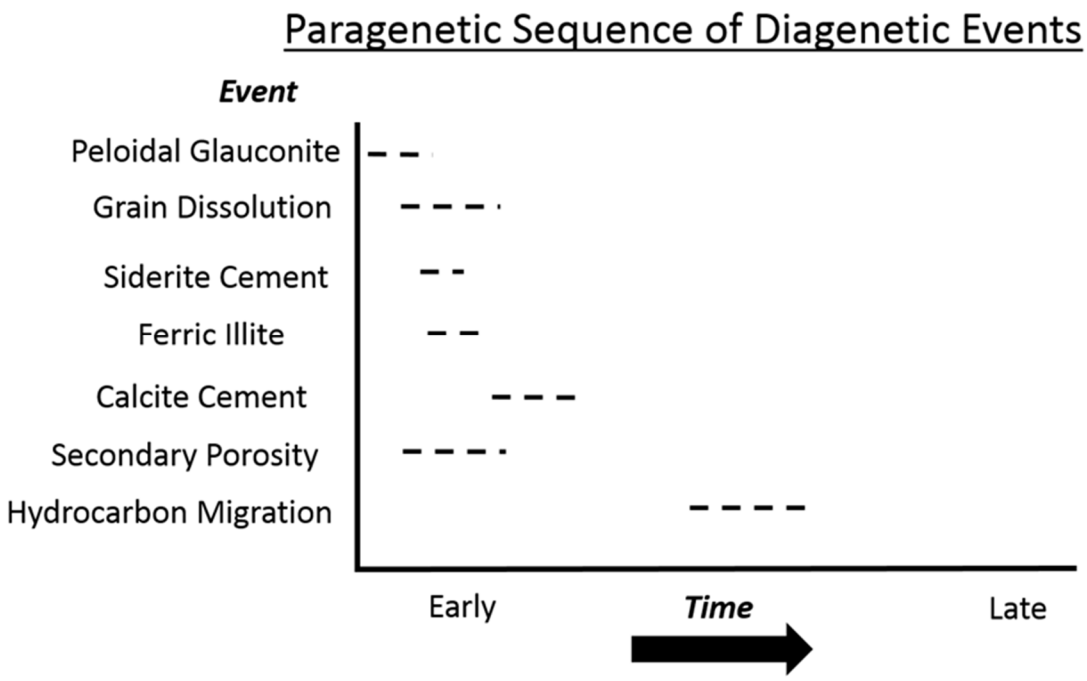

Figure 42. Illustrating the possible paragenetic sequence of diagenetic events of the Eutaw Formation, eastern Gilbertown field.

The hypothesis that bypassed pay exists in the Eutaw Formation has been examined by integrating the results of petrology, well analysis, and core analysis. Well log signatures could not be correlated with changes in oil saturation. Changes in resistivity most commonly reflect changes of porosity and glauconite content rather than changes in fluid saturation of the uninvaded zone, as scatterplots of oil and resistivity values had extremely low coefficients of determination (< 0.1). Core analysis and production data, however, reveal oil saturation occurs in sandstone with low resistivity that has been overlooked. ROIP in eastern Gilbertown Field could be as high as 70.4 MMbbl, considering that the original oil-in-place values are approximately 82.4 million barrels of oil and the eastern part of the field has produced nearly 12 million barrels of oil. This result indicates that only 15% of OOIP has been recovered. Figure 43 is a bubble map of the percent of OOIP recovered by each well. Interestingly, recovery is highest (40-50%) in two wells perforated only in interval E7 in the southwest area of the faulted anticline. Three wells in the horst adjacent to fault EGA and one well just west of the horst have recovered 30-

40% of the original oil-in-place. These wells are completed in the lower intervals with high permeability values (E2-E4). Most wells in eastern Gilbertown Field have produced less than 30% of OOIP. The length of time each well has produced, the number of intervals perforated, and the heterogeneity of the reservoir are all factors that could affect recovery.

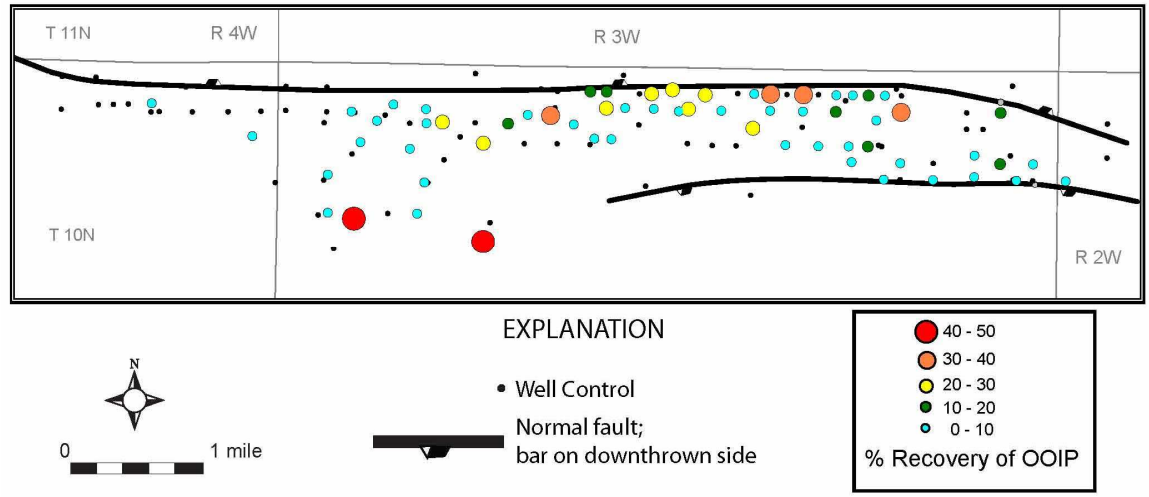

Figure 43. Map of eastern Gilbertown Field showing percent recovery of Eutaw Formation based on production data and OOIP estimates.

Comparing perforated intervals to OOIP raises several questions. Interval E6, which has the greatest OOIP values in the formation, was completed in few wells high on the eastern Gilbertown structure (Figs. 35, 44). Core analyses data demonstrate that sandstone in interval E6 has lower permeability than intervals E1, E2, E3, and E4, all of which produce high on the structure (Figs. 26, 27). Thin section analysis indicates that high percentages of glauconite and calcite are the principal causes of reduced permeability. It is also possible that where perforation zones were chosen from well logs alone, the low resistivity and more positive SP characteristic did not look as attractive as some of the lower intervals that contain less glauconite and carbonate cement (Fig. 44). Interval E6 has the highest values of OOIP and yet has been completed the least in the horst because of shaly reservoir. However, applying directional drilling and hydraulic fracturing technology in a manner similar to what is now common in tight reservoirs could

provide a great opportunity for future development. Interval E4 was perforated in very few wells in the central area of the horst, where interval E3 is very productive. Considering that interval E4 is structurally higher than E3, it may be an attractive target for completion (Fig. 44).

Aside from the two areas that were unitized for waterflood, the field appears to have been primarily developed with a variety of well spacings. Due to the low API gravity of the oil (17-20°), efficient drainage may necessitate well spacing much closer than current wells, especially in the upper sandstone intervals. Accordingly, infill drilling appears to be a promising approach for future development, and reservoir models may provide insight on optimal well spacing. Pashin et al. (2000) noted that many wells were commonly not completed in intervals that were perforated in offset wells. Hence, significant pay appears to remain behind casing, and opportunities may exist to complete untapped pay in existing wells (Fig. 44). The majority of the wells at Gilbertown Field have now been plugged, but likely could be reentered at nominal cost. Considering the shallow depth of the formation, it may be cost effective to drill new wells into the Eutaw Formation rather than working with the plugged wells, and directional drilling may facilitate contact of bypassed pay, particularly in zones with reduced permeability. Structural cross sections in Figure 44 display the pattern of perforated intervals, as well as those sandstones with behind the pipe potential. There are many more examples of pay that has been bypassed in the eastern part of Gilbertown Field.

No wells completed in the Eutaw Formation in eastern Gilbertown Field have a record of being hydrofractured. Fracture stimulation may improve recovery by extending the reach of existing wells and thus contacting untapped and bypassed pay, although a significant risk is contact of high-permeability streaks that are already depleted and watered out. As mentioned above directional drilling could also have potential for revitalization of the field, and multilateral drilling techniques may improve the efficiency of recovery operations. Care needs to be taken, however, to avoid water-bearing zones that may constitute thief zones that would dilute the oil recovered from untapped or bypassed pay intervals.

Other methods that may be considered include open-hole completions. For example, the Northeast Butterly Field in Garvin County, Oklahoma produces from unconsolidated Ordovician sand, and testing was performed to compare perforated cased-hole completions versus open-hole completions (Phillips and Whitt, 1986). The wells produce primarily oil in the first few months and then produced mainly water. Sand production increased along with the water production, but numerous wells in Gilbertown employ progressive cavity pumps, which are built to pass fines. The open-hole completions in Northeast Butterfly Field resulted in reduced water channeling and increased the reach of the oil sweep (Phillips and Whitt, 1986). However, open-hole conpletions may exacerbate inefficient oil sweep related to high-permeability thief zones in the Eutaw Formation, and so zone isolation in attempt to avoid or minimize the impact of these streaks would be critical. One option would be to reenter existing wells and mill the casing and cement in untapped pay intervals that are not in close proximity to known or suspected thief zones.

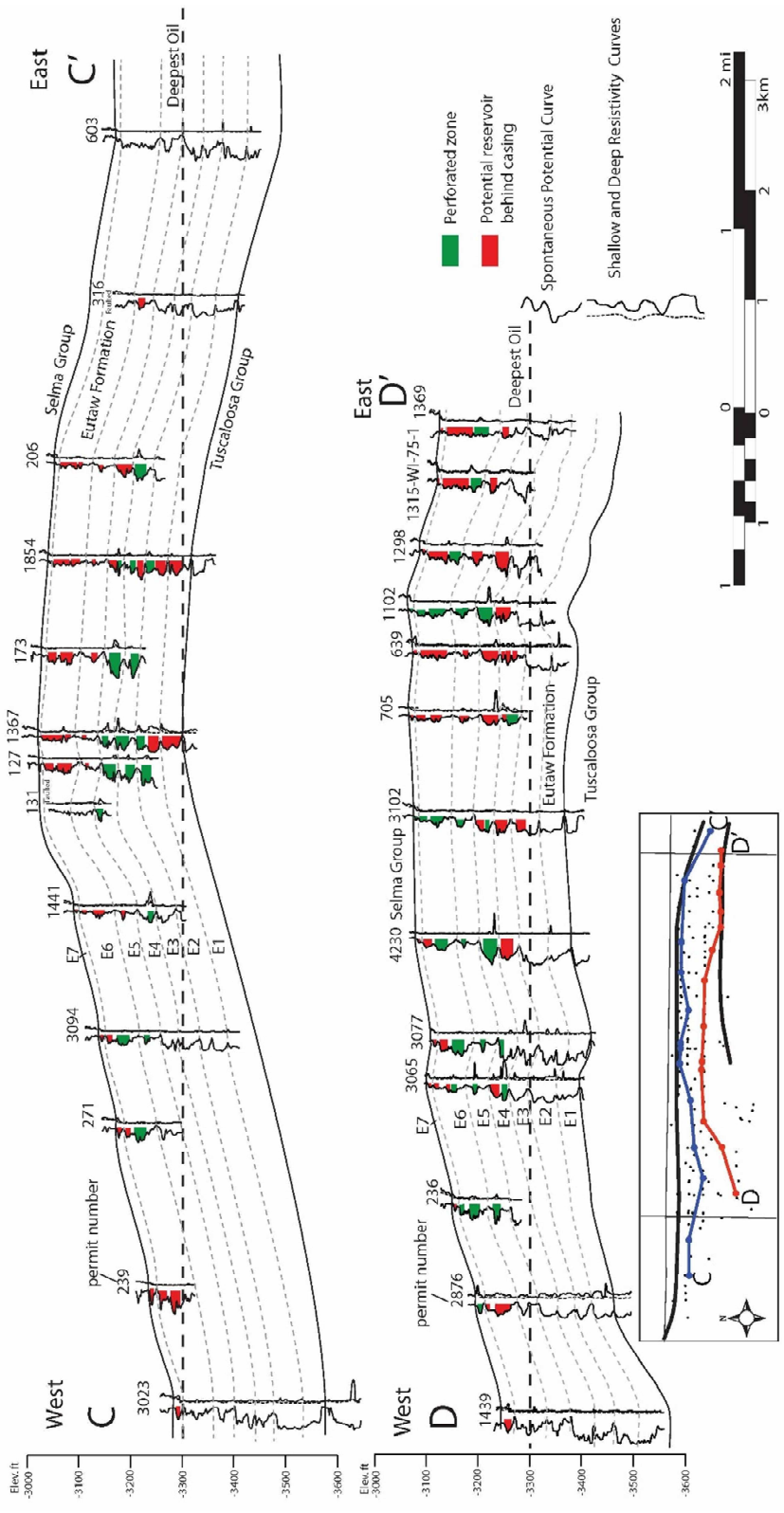

Figure 44. Structural cross sections C-C' and D-D' showing perforated intervals and potential recompletion targets in eastern Gilbertown Field and map showing location of cross sections.

Thief zones need to be taken into acccount when considering the viability of waterflooding efforts. Production from the wells in the two waterflood units did not show a great increase in production following unitization, but waterflooding did consistently flatten decline curves. The East Gilbertown Eutaw Unit produced from interval E6, and was shut down in 1999 after producing successfully for 25 years (Fig. 45). The Gilbertown (Eutaw Sand) Unit, which is adjacent to Fault EGA, is still operational. However, no production data have been posted since June 2016 (Fig. 45). The Gilbertown (Eutaw Sand) Unit is primarily producing from intervals E2, E3, and E4, and it has been successful even though these intervals contain Darcy-class permeability streaks in the waterflood area (Fig. 23). This could be very problematic for continuing waterflood efforts, as injecting near these streaks likely inhibits oil sweep. Moreover, it is difficult to find these zones without core analysis. Greer (1995) listed several fields in eastern Mississippi that, like Gilbertown, have a history of oil production from the Eutaw Formation. Four of these fields have been waterflooded successfully in addition to the two units in eastern Gilbertown Field.

CO_2 and other gases may be injected to facilitate pressure sweep, but the low API gravity of the oil precludes the possiblity of miscible tertiary recovery. CO_2 would arguably penetrate a lot of spaces that water could not. Thermal recovery methods also could be effective at Gilbertown Field, although economic analysis indicates that it is currently too expensive (Charles D. Haynes, personal communication).

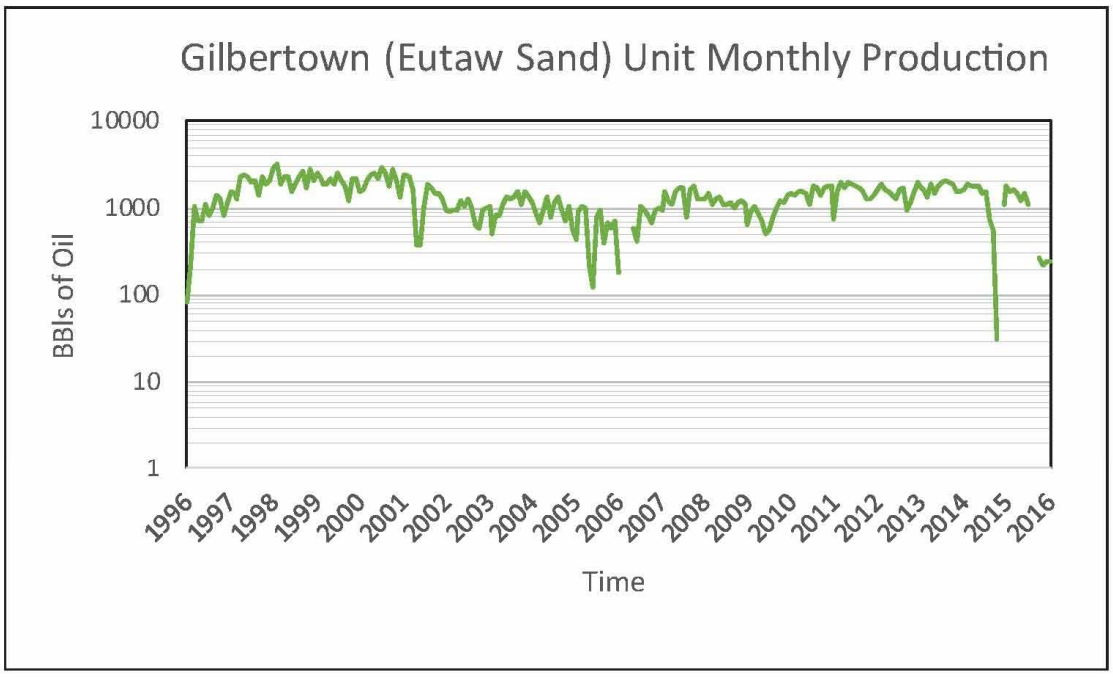

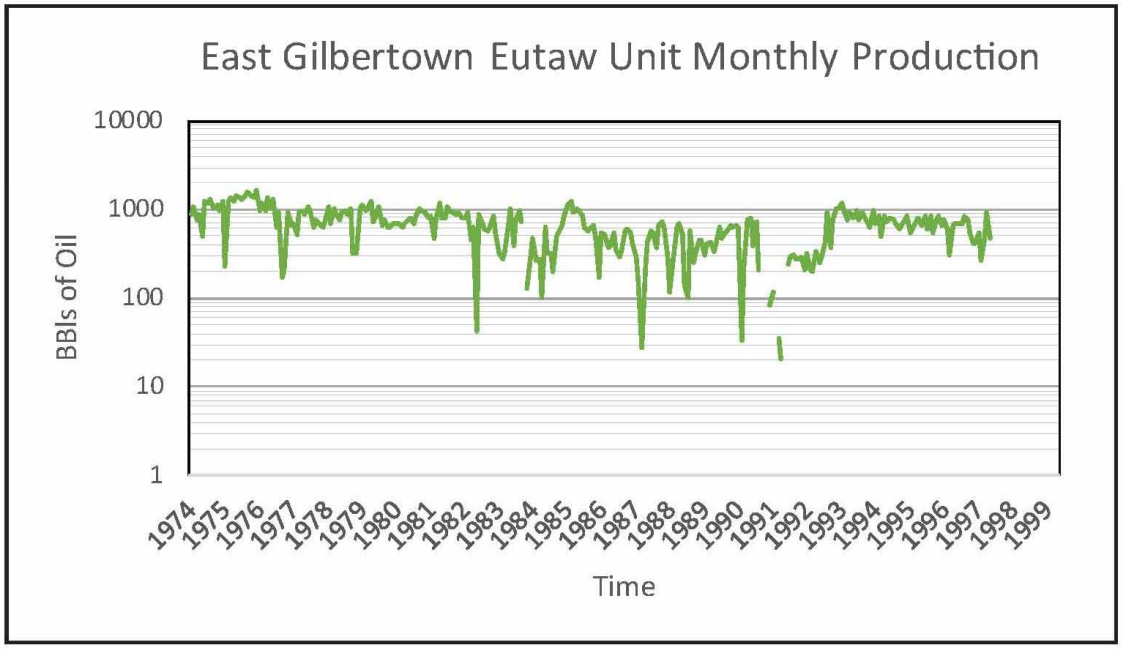

Figure 45. Decline curves of units producing from Eutaw Formation at eastern Gilbertown Field.

CHAPTER VI

CONCLUSIONS

The hypothesis that bypassed pay exists in the Eutaw Formation at Gilbertown Field has been tested by integrating core analyses, thin section alaysis, and well log analysis. Nearly 85% of OOIP in eastern Gilbertown Field remains in place (ROIP ~70 MMbbl). It is likely that revitalization of the field through recompletion, infill drilling, and secondary recovery efforts, that oil recovery can be improved significantly. Indeed, recoverability of an additional 5% of OOIP would constitute a reserve expansion of more than 4 MMbbl. The interval with the highest OOIP, interval E6, has been perforated in very few wells near the crest of the structure where results from core analyses show high oil percentages, and permeability values of 50 mD. This interval could have the most upside potential, and directional drilling and hydraulic fracturing may help maximize recovery. Bypassed oil was observed throughout eastern Gilbertown Field, and recompletion targets are plentiful.

REFERENCES

Amorosi, A., and Centineo, M. C., 1997, Glaucony from the Eocene of the Isle of Wight (southern UK): implications for basin analysis: Geological Society of London, Journal, v. 154, p. 887-896.

Asquith, G.B., 1990, Log Evaluation of Shaly Sandstone Reservoirs: A Practical Guide: Tulsa, OK, American Association of Petroleum Geologists continuing education course note series 31, 59p.

Bailey, R. J., and Atherton, M. P., The petrology of a glauconitic sandy chalk: Journal of Sedimentary Petrology, v. 39, p. 1420-1431.

Berner, R. A., 1981, A new geochemical classification of sedimentary environments: Journal of Sedimentary Petrology, v. 51, p. 359-365.

Chaudhuri, A. K., Chanda, S.K., and Dasgupta, Somnath, 1994, Proterozoic glauconitic peloids from south India: Their origin and significance: Journal of Sedimentary Research, v. A64, p. 765-770.

Cloud, P. E., Jr., 1955, Physical limits of glauconite formation: American Association of Petroleum Geologist Bulletin, v. 39, p. 484-492.

Coleman, M. L., 1985, Geochemistry of diagenetic non-silicate minerals: Kinetic consideration: Philosophical Transactions of the Royal Society of London, v. A-315, p. 39-56.

Cook, M. R., 1993, The Eutaw aquifer in Alabama: Alabama Geological Survey Bulletin 156, 105 p.

Cook, P. L., Jr., Schneeflock, R. D., Bush, J. D., and Marble, J. C., 1990, Trimble field, Miss.: 100 Bcf of bypassed, low resistivity Cretaceous Eutaw pay at 7,000 ft: Oil & Gas Journal, Oct. 22, 1990, p. 96-102.

Current, A. M., 1948, Gilbertown Field, Choctaw County, Alabama: Tulsa, Oklahoma, American Association of Petroleum Geologists, Structure of Typical American Oil Fields, v. 3, p. 1-4.

Curtis, C. D., and Coleman, M. L., 1986, Controls of the precipitation of early diagenetic calcite, dolomite, and siderite concretions in complex depositional sequences, *in* Gautier, D. L., ed., Roles of organic matter in sediment diagenesis: Society of Economic Paleontologists and Mineralogists Special Publication 38, p. 23-33.

Dasgupta, Somnath, Chaudhuri, A. K., and Fukuoka, Masato, 1990, Compositional characteristics of glauconitic alterations of K-feldspar from India and their implications: Journal of Sedimentary Petrology, v. 60, p. 277-287.

Frascogna, X. M., 1957, Gilbertown and East Gilbertown Field Choctaw County, Alabama: Mesozoic-Paleozoic Producing Areas of Mississippi and Alabama, v. 1, Jackson, Mississippi Geological Society, p. 50-53.

Frazier, W. J., and Taylor, R. S., 1980, Facies changes and paleogeographic interpretations of the Eutaw Formation (Upper Cretaceous) from western Georgia to central Alabama, in Tull, J.F., ed., Field Trips for the Southeastern Section of the Geological Society of America, Birmingham, Alabama, p. 1-27.

Galliher, E. W., 1935, Glauconite genesis: Geological Society of America Bulletin, v. 46,p. 1351-1366.

Greer, B. R., 1995, Deposition and remaining productive capabilities of the Upper Cretaceous Eutaw sands of east-central Mississippi: Gulf Coast Association of Geological Societies Transactions, v. 45, p.229-235.

Guohai Jin and Groshong, R. H., Jr., 2006, Trishear kinematic modeling of extensional drag folding, Journal of Structural Geology, v. 28, p. 170-183.

Guohai Jin, Groshong, R. H., Jr., and Pashin, J. C., 2009, Growth trishear model and its application to the Gilbertown graben system, southwest Alabama: Journal of Structural Geology, v. 31, p. 926-940.

Guohai Jin, Groshong, R. H., Jr., and Pashin, J. C., 1999, Relationship between drag fold geometry and fracture production in the Selma Chalk, Gilbertown oil field, southwest Alabama: Gulf Coast Association of Geological Societies Transactions, v. 49, p. 17-18.

Hilchie, D.W., 1979, Old electric log interpretation (Pre-1958): American Association of Petroleum Geologists Methods in Exploration Series 15, 107 p.

Horton, J. W., Zietz, Isidore, and Neathery, T. L., 1984, Truncation of the Appalachian Piedmont beneath the Coastal Plain of Alabama: Geology, v. 12, p. 51-55.

Jiafu Qi, Pashin, J. C., and Groshong, R. H., Jr., 1998, Structure and evolution of North Choctaw Ridge Field, Alabama, a salt-related footwall uplift along the peripheral fault system, Gulf Coast basin: Gulf Coast Association of Geological Societies Transactions, v. 48, p. 349-359.

Light, M. A., 1952, Evidence of authigenic and detrital glauconite: Science, v. 115, no. 2977, p. 73-75.

Mancini, E.A., Li, P., Goddard, D.A. and Zimmerman, R.K., 2005, Petroleum source rocks of the onshore interior salt basins, north central and northeastern Gulf of Mexico: Gulf Coast Association of Geological Societies Transactions, v. 55, p. 486-504.

Mancini, E. A., and Tew, B. H., 1991, Relationships of Paleogene stage and planktonic foraminiferal zone boundaries to lithostratigraphic and allostratigraphic contacts in the eastern Gulf Coastal Plain: Journal of Foraminiferal Research, v. 21, p. 48-66.

Mann, S. D., and Kopaska-Merkel, D. C., 1992, Depositional History of the Smackover-Buckner Transition, Eastern Mississippi Interior Salt Basin: Gulf Coast Association of Geological Societies Transactions, v. 42, p. 245-265.

Mozley, P. S. and Wersin, P., 1992, Isotopic composition of siderite as an indicator of depositional environment: Geology, v. 20, p. 817-820.

Pashin, J. C., Groshong, R. H., Jr., and Guohai Jin, 1998, Structural modeling of a fractured chalk reservoir: toward revitalizing Gilbertown Field, Choctaw County, Alabama: Gulf Coast Association of Geological Societies Transactions, v. 48, p. 335-347.

Odin, G. S., and Matter, A., 1981, De glauconiarum origine: Sedimentology, v. 20, p. 611-641.

Odom, E., 1984, Glauconite and celadonite minerals, in Baile, S. W., ed., Reviews in Mineralogy, v. 13, p. 545-572.

Pashin, J. C., Groshong, R. H., Jr., and Guohai Jin, 1998, Structural modeling of a fractured chalk reservoir: toward revitalizing Gilbertown Field, Choctaw County, Alabama: Gulf Coast Association of Geological Societies Transactions, v. 48, p. 335-347.

Pashin, J. C., Raymond, D. E., Alabi, G. G., Groshong, R. H., Jr., and Guohai Jin, 2000, Revitalizing Gilbertown oil field: Characterization of fractured chalk and glauconitic sandstone reservoirs in an extensional fault system: Alabama Geological Survey Bulletin 168, 81 p.

Phillips, F.L. and Whitt, S.R., 1986, Success of openhole completions in the Northeast Butterly Field, southern Oklahoma: SPE Production Engineering, v. 1, p.169-173.

Salvador, Amos, 1987, Late Triassic-Jurassic paleogeography and origin of the Gulf of Mexico basin: American Association of Petroleum Geologists Bulletin, v. 71, p. 419-451.

Schmidt, V. and McDonald, D.A., 1979, Secondary reservoir porosity in the course of sandstone diagenesis: Society of Economic Paleontologist and Mineralogists Special Publication 26, p. 175-207.

Takashi, J., 1939, Synopsis of glauconization, in Trask, P.D, ed., Recent marine sediments: Tulsa, American Association of Petroleum Geologists, p. 503-513.

Velde, B., 1985, On the origin of glauconite and chamosite granules: Geo-Marine Letters, v. 5, p. 47-49.

Walsh, J.W., Brown, S.L. and Asquith, G.B., 1993, Analyzing Old electric logs in shaly sand formations: Society of Petroleum Engineers, SPE-25508-MS, 8p.

Worrall, D. M., and Snelson, S., 1989, Evolution of the northern Gulf of Mexico, with emphasis on Cenozoic growth faulting and the role of salt, in Bally, A. W., and Palmer, A. R., eds., The geology of North America; and overview: Boulder, Colorado, Geological Society of America, The Geology of North America, Volume A, p. 97-138.

Worthington, P.F. 2000, Recognition and evaluation of low-resistivity pay: Petroleum Geoscience, v. 6, p. 77-92.

VITA

Bradley Joseph Jackson

Candidate for the Degree of

Master of Science

Thesis: AN INTEGRATED APPROACH TO STRATIGRAPHIC ARCHITECTURE AND RESERVOIR ANALYSIS OF THE EUTAW FORMATION: EASTERN GILBERTOWN FIELD, ALABAMA

Major Field: Geology

Biographical:

Education:

Completed the requirements for the Master of Science in Geology at Oklahoma State University, Stillwater, Oklahoma in May 2017.

Completed the requirements for the Bachelor of Science in Geology at Oklahoma State University, Stillwater, Oklahoma in 2013.

Completed the requirements for the Associate of Science in Pre-engineering at Carl Albert State College, Poteau, Oklahoma in 2011.

Experience: Internship at Linn Energy (1 summer), Geologist at Territory Resources, LLC (1 year)

Professional Memberships: AAPG, OCGS, TGS, GSA